Techno-Economic Assessment of Optimised Vacuum Swing Adsorption for Post-Combustion CO_2 Capture from Steam-Methane Reformer Flue Gas

Sai Gokul Subraveti[a], Simon Roussanaly[b,*], Rahul Anantharaman[b], Luca Riboldi[b], Arvind Rajendran[a,*]

[a]*Department of Chemical and Materials Engineering, University of Alberta, 12th floor, Donadeo Innovation Centre for Engineering (ICE), 9211-116 Street, Edmonton, Alberta T6G1H9, Canada*
[b]*SINTEF Energy Research, NO-7465, Trondheim, Norway*

Abstract

This study focuses on the techno-economic assessment integrated with detailed optimisation of a four step vacuum swing adsorption (VSA) process for post-combustion CO_2 capture and storage (CCS) from steam-methane reformer dried flue gas containing 20 mol% CO_2. The comprehensive techno-economic optimisation model developed herein takes into account VSA process model, peripheral component models, vacuum pump performance, scale-up, process scheduling and a thorough cost model. Three adsorbents, namely, Zeolite 13X (current benchmark material for CO_2 capture) and two metal-organic frameworks, UTSA-16 (widely studied metal-organic framework for CO_2 capture) and IISERP MOF2 (good performer in recent findings) are optimised to minimise the CO_2 capture cost. Monoethanolamine (MEA)-based absorption technology serves as a baseline case to assess and compare optimal techno-economic performances of VSA technology for three adsorbents. The results show that the four step VSA process with IISERP MOF2 outperforms other two adsorbents with a lowest CO_2 capture cost (including flue gas pre-treatment) of 33.6 € per tonne of CO_2 avoided and an associated CO_2 avoided cost of 73.0 € per tonne of CO_2

This is the accepted version of an article published in Separation and Purification Technology
http://dx.doi.org/10.1016/j.seppur.2020.117832

avoided. Zeolite 13X and UTSA-16 resulted in CO_2 avoided costs of 90.9 and 104.9 € per tonne of CO_2 avoided, respectively. The CO_2 avoided costs obtained for the VSA technology remain higher than that of the baseline MEA-based absorption process which was found to be 66.6 € per tonne of CO_2 avoided. The study also demonstrates the importance of using cost as means of evaluating the separation technique compared to the use of process performance indicators. Accounting for the efficiency of vacuum pumps and the cost of novel materials such as metal-organic frameworks is highlighted.

Keywords: carbon dioxide capture and storage, vacuum swing adsorption, techno-economic analysis, steam-methane reformer, optimisation, metal-organic frameworks

*Corresponding authors
Email addresses: Simon.Roussanaly@sintef.no (Simon Roussanaly), arvind.rajendran@ualberta.ca (Arvind Rajendran)

1. Introduction

Hydrogen is a clean fuel that plays an important role in transition towards a low-carbon sustainable energy future. With growing demands in various sectors such as, power, heating, industry, transportation, global hydrogen production is expected to substantially increase in the next few decades [1]. Although hydrogen can be produced through renewable sources, over 95% of the global hydrogen production relies on fossil fuels [1, 2]. Since this production route involves high CO_2 emissions, CO_2 capture and storage (CCS) is a path forward to enable large scale hydrogen production with low-carbon emissions in hydrogen plants to meet growing demands. Steam-methane reforming (SMR) of natural gas continues to be the leading technology for large-scale hydrogen production [3] which accounts for almost 50% of the hydrogen produced globally [4]. In SMR-based hydrogen plants, natural gas undergoes steam-reforming followed by water-gas shift to obtain shifted syngas. Owing to the highly endothermic reforming reactions, combustion of natural gas in the reformer remains inevitable [3]. Pressure swing adsorption (PSA) then purifies the shifted syngas to produce ultrapure hydrogen. Based on aforementioned process steps, CO_2 sources can be associated to SMR furnace flue gas and shifted syngas from reforming and water-gas shift reactions. While up to 60% CO_2 can be captured from shifted syngas [1], post-combustion CO_2 capture from SMR furnace flue gas must be deployed to achieve higher overall capture rates from SMR-based hydrogen plants [3] and thus enabling low-carbon footprint hydrogen. The current state-of-the-art separation technology for post-combustion CO_2 capture in SMR plants involves monoethanolamine (MEA) based absorption [3].

This is the accepted version of an article published in Separation and Purification Technology
http://dx.doi.org/10.1016/j.seppur.2020.117832

Alternative post-combustion CO_2 capture technologies such as, membrane separation and vacuum swing adsorption (VSA) have emerged as promising technologies that are currently in the R&D stage [5]. The VSA technology was also commercially demonstrated for CO_2 capture from syngas in a SMR-based plant at Valero Port Arthur Refinery (Texas, USA) [6]. With growing interest to develop adsorption technology for CO_2 capture, major improvements have been made to develop new adsorbents and processes [5]. Recent model-based material screening studies have enabled the discovery of potential adsorbents for CO_2 capture applications [7, 8, 9, 10]. Alongside, novel processes that are efficient in terms of energy and productivity are being developed [11]. It is worth noting that majority of studies in the literature focus on the development of materials. Most process studies have focused either on the development of novel processes or the screening/evaluation of adsorbents. These studies often perform assessments based on process metrics such as parasitic energy consumption and/or productivity. While these are important metrics, they seldom provide an idea of the cost of capture. Without a proper estimate of the cost, it is problematic to compare various technologies, evaluate the complexities involved in scale-up, etc. Hence, it is important that process studies go beyond the evaluation of process metrics and consider the cost of capture. Such detailed analyses are not common in the literature, with a few exceptions that are discussed here.

Table 1 summarizes a sample of relevant techno-economic studies that focused on P/VSA technology for post-combustion CO_2 capture. As can be seen from the table, many studies have focused mainly on coal-fired power plants and there are no studies reported for post-combustion CO_2 capture in hydrogen plants using the VSA technology. Most previous

This is the accepted version of an article published in Separation and Purification Technology
http://dx.doi.org/10.1016/j.seppur.2020.117832

studies also overlooked the dynamics of the vacuum pump in P/VSA simulations which can lead to two major concerns. Typically, predefined pressure histories used to approximate the dynamics of vacuum pumps can significantly overestimate the productivity of the capture plant. Another shortcoming comes from the assumption of high vacuum pump efficiencies to calculate the VSA energy consumption. This is a critical aspect since the production of high purity CO_2 at high recovery requires very low vacuum pressures at which pump efficiencies are known to drop dramatically [18, 19]. Practical considerations on the vacuum pump performance are often omitted in cost estimations. Previous research has not considered the scale-up and proper column scheduling in their optimal cost estimations with notable exception being the work of Khurana and Farooq [16]. Given the complexity of CO_2 capture problem, multiple trains of VSA columns are required to treat the flue gas. Under such circumstances, it is important to carefully perform the column scheduling and the scale-up to ensure continuous feed. One more limitation relates to the adsorbent cost. As can be seen from Table 1, some studies estimated the costs of novel adsorbents such as metal-organic frameworks to be the same as that of Zeolite 13X. This assumption may no longer be valid, especially when the raw materials used to synthesize these adsorbents are expensive. Further, a wide range of financial parameters were used for cost estimations which makes the comparison of VSA performance with other technologies challenging. The P/VSA cost estimations are not straightforward and the literature has not rigorously assessed the techno-economics apart from the work of Khurana and Farooq [16]. Therefore, a detailed cost model based on established financial guidelines together with the full complexity of VSA remains essential in order to compare VSA with other capture technologies. Improvements in VSA

This is the accepted version of an article published in Separation and Purification Technology
http://dx.doi.org/10.1016/j.seppur.2020.117832

modelling in recent years to perform reliable calculations is another factor to consider for the need of up to date cost estimation. In order to enable cost-efficient designs, integrating the detailed cost model with the design and optimisation is essential [20].

This is the accepted version of an article published in Separation and Purification Technology
http://dx.doi.org/10.1016/j.seppur.2020.117832

Table 1: Summary of selected techno-economic studies for P/VSA.

Study	Case/Application	CO_2 composition	Process	Adsorbent(s)	KPI[a]	Lowest CO_2 Capture Cost	Scale-up/Scheduling	MOF Cost	Purity/Recovery Constraints	Comments
Ho et al. (2008) [12]	500 MW power plant	13%	Skarstorm PSA/VSA	Zeolite 13X	CO_2 avoided cost	US$51 per ton of CO_2 avoided	Simple	-	None	Short-cut model with many simplifying assumptions Preliminary analysis which is only indicative
Hasan et al. (2012) [13]	Generic	Wide range	4-step PSA/VSA	Zeolite 13X	Total annualized cost	Wide range	No	-	90%/90%	Vacuum pump dynamics not considered Column scheduling and scale-up not considered
Susarla et al. (2015) [14]	500 MW power plant	15%	4-step PVSA	Zeolite 13X	Total annualized cost	US$33.4 per tonne of CO_2 avoided	Extensive	-	90%/90%	Dry flue gas considered
Leperi et al. (2016) [15]	30 MW coal power plant	14.1%	Two-stage modified Skarstorm cycle	Zeolite 13X Zeolite 5A Ni-MOF-74 HKUST-1	Total annualized cost	US$ 34.1 per ton of CO_2 captured	No	Based on metal prices	90%/90%	Small-scale power plant No column scheduling
Khurana & Farooq (2019) [16]	550 MW power plant	15%	4-step VSA 6-step VSA	Zeolite 13X UTSA-16 Min. cost adsorbent	Levelized cost of electricity	US$26.3 per tonne of CO_2 avoided	Extensive	Fixed to Zeolite 13X	95%/90%	Based on a dry flue gas Framework also facilitates the search for the lowest cost adsorbent MOF costs assumed to be same as that of the Zeolite 13X
Danaci et al. (2020) [17]	400 MW natural gas power plant 500 MW coal power plant 1 MM TPA cement plant 4 MM TPA steel plant	4.38% 12.5% 21% 25.5%	3-step VSA	25 Adsorbents incl. UTSA-16, Zeolite 13X	Annualized capture cost	Wide range	No	Fixed to Zeolite 13X	None	Simplified VSA model that does not consider column dynamics MOF cost estimations based on bulk metal prices performed for UTSA-16
This work	450 TPD SMR H_2 plant	20%	4-step VSA	Zeolite 13X UTSA-16 IISERP MOF2	CO_2 avoided cost	33.6 € per tonne of CO_2 avoided	Extensive	Based on metal prices	95%/90%	Vacuum pump performance incorporated into VSA simulation Adsorbent manufacturing factor considered in estimating MOF costs Comprehensive cost model consistent with best practices

[a]Key Performance Indicator

In the present work, an integrated techno-economic optimisation model is developed that takes into account detailed VSA process model, peripheral component models, vacuum pump performance and a comprehensive costing model. This model is used to assess the techno-economic performance of an optimised VSA process for post-combustion CO_2 capture in SMR-based hydrogen plants. Three different adsorbents are evaluated for their technical and cost performances based on a four step VSA cycle with light product pressurisation and tested for their competitiveness by comparing with state-of-the-art MEA-based absorption. In addition, different optimisation cases are considered to highlight (1) the critical choice of process design objectives, (2) the importance of incorporating vacuum pump performance into the techno-economic optimisation model, (3) the effect of adsorption column sizing and (4) the influence of adsorbent costs.

2. Case Study

The SMR process for hydrogen production without CO_2 capture considered in this study is based on a single steam-methane reforming train with a production capacity of 450 tonnes of hydrogen per day. A simplified process flow diagram of the SMR-based hydrogen production system is shown in Fig. 1. First, natural gas is converted to syngas through a pre-reformer and a reformer. After the reformer, the CO in the syngas is converted to CO_2 through a high-temperature and a low-temperature water-gas shift. It is also worth noting that the water-gas shift enables the production of HP steam used to generate electricity. A PSA unit then separates H_2 from the rest of converted syngas to produce high purity hydrogen (main product of the plant). The PSA tail gas is sent back to the furnace to burn

This is the accepted version of an article published in Separation and Purification Technology
http://dx.doi.org/10.1016/j.seppur.2020.117832

with the natural gas and deliver heat for the reforming process. Without CO_2 capture, the hydrogen plant results in an exhaust flue gas of 233.9 kg/s at 1.02 bar and 353.15 K and the following molar composition: 16.23% CO_2, 63.31% N_2, 17.87% H_2O, 1.84% O_2, 0.75% Ar [21]. The scope of this work is identified in Fig. 1.

To benchmark the adsorption-based process, a standard monoethanol amine-based (MEA) CO_2 capture is considered as the reference technology as illustrated in Fig. S1 in the Supporting Information. After CO_2 capture, the CO_2 is pressurised to 200 bar before being transported to an offshore saline aquifer located 140 km away. While a summary of the performances of the hydrogen plant with and without MEA-based CCS is presented in Table S1 in the Supporting Information, more details can be found elsewhere [21].

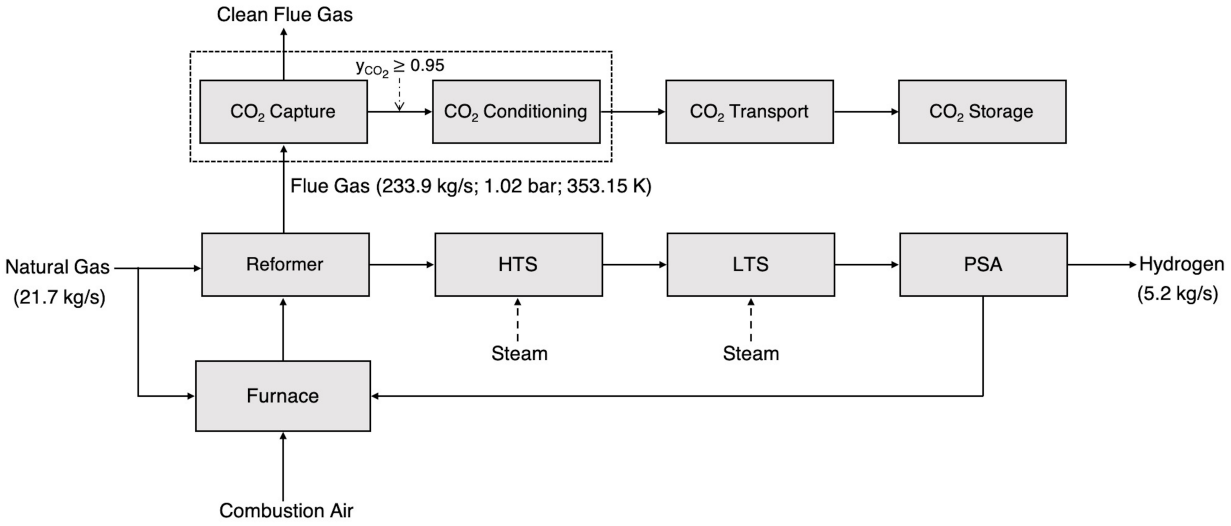

Figure 1: Process flow diagram of the hydrogen production plant and the overview of CCS chain. The dotted box represents the scope of the study.

This is the accepted version of an article published in Separation and Purification Technology
http://dx.doi.org/10.1016/j.seppur.2020.117832

3. Systematic Design of VSA Systems

An integrated techno-economic optimisation framework is proposed for the design of VSA processes. Most VSA studies for CO_2 capture deal with process optimisations either involving energy reduction or productivity maximization or both. While these are good proxies for operating and capital costs, the true estimate of a technology should be based on a thorough techno-economic study that accurately incorporates the trade-offs involved. In this work, a techno-economic analysis coupled with a rigorous process optimisation approach is used. The key features of this approach are following:

1. The use of a process cycle that has been demonstrated at a pilot plant facility to produce high CO_2 purity and recovery.
2. Rigorous modelling of the adsorption process that explicitly accounts for full transient column dynamics and cyclic-steady state performance of the process.
3. Rational scale-up approach that determines the number of columns and parallel trains to ensure continuous operation.
4. A costing framework that is consistent with best practices in order to improve the reliability of the cost values.

The framework used for this study is illustrated in Fig. 2. The inputs to this framework are technical and economic design basis, VSA cycle and physiochemical properties such as adsorption isotherms. Based on the inputs provided, integrated simulation and costing framework coupled with stochastic optimisation outputs the cost optimal design of the VSA process. More details of these components are presented below.

This is the accepted version of an article published in Separation and Purification Technology
http://dx.doi.org/10.1016/j.seppur.2020.117832

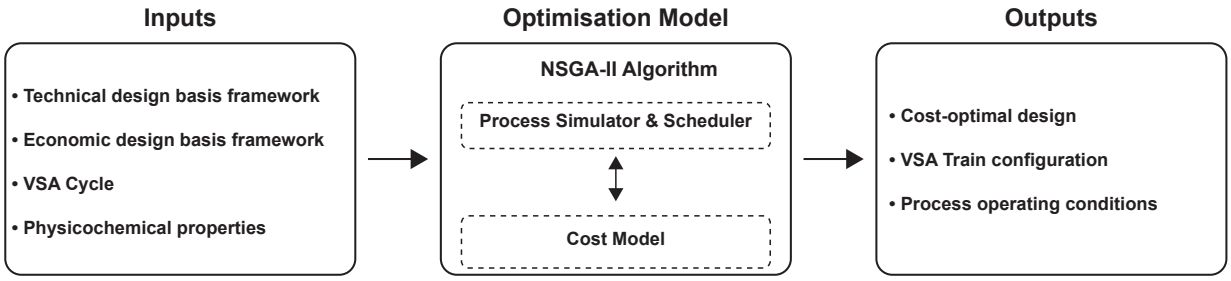

Figure 2: Integrated techno-economic optimisation methodology.

3.1. VSA Capture System

3.1.1. Process Layout

The process layout of adsorption-based CO_2 capture is illustrated in Fig. 3. Given the detrimental nature of water on many adsorbents, the wet flue gas of the hydrogen plant is first cooled to 313.15 K by a direct contact cooler and then dehydrated using a molecular sieve to remove the water [20]. The dry flue gas requires compression to overcome the pressure drop in VSA columns. Two identical single-stage compressors are employed to compress the entire dry flue gas to the desired pressures. Coolers follow each compression unit to cool the feed mixture to 298.15 K.

A feed header splits the dry flue gas as feed into M identical VSA units [14]. The feed mixture to VSA units is considered to contain 20% CO_2, 77% N_2, 2% O_2, 1% Ar. For simplicity, a binary mixture of 20% CO_2 and 80% N_2 was used to simulate the VSA process. This can be justified by the fact that both O_2 and Ar adsorb weaker than N_2 on most adsorbents, specifically those considered in this study and hence, can be considered to be adequately represented by N_2. Each VSA unit consists of N identical columns operating out of phase to implement the cycle operation. Several switching valves, dedicated vacuum

This is the accepted version of an article published in Separation and Purification Technology
http://dx.doi.org/10.1016/j.seppur.2020.117832

pumps are employed to remove N_2 and collect CO_2 separately. The CO_2 after capture undergoes a multi-stage compression with intercooling from 1 bar and 298.15 K to the target conditions prior offshore pipeline transport (200 bar and 318.15 K). More details on technical modelling of various peripheral components are summarized in the Supporting Information.

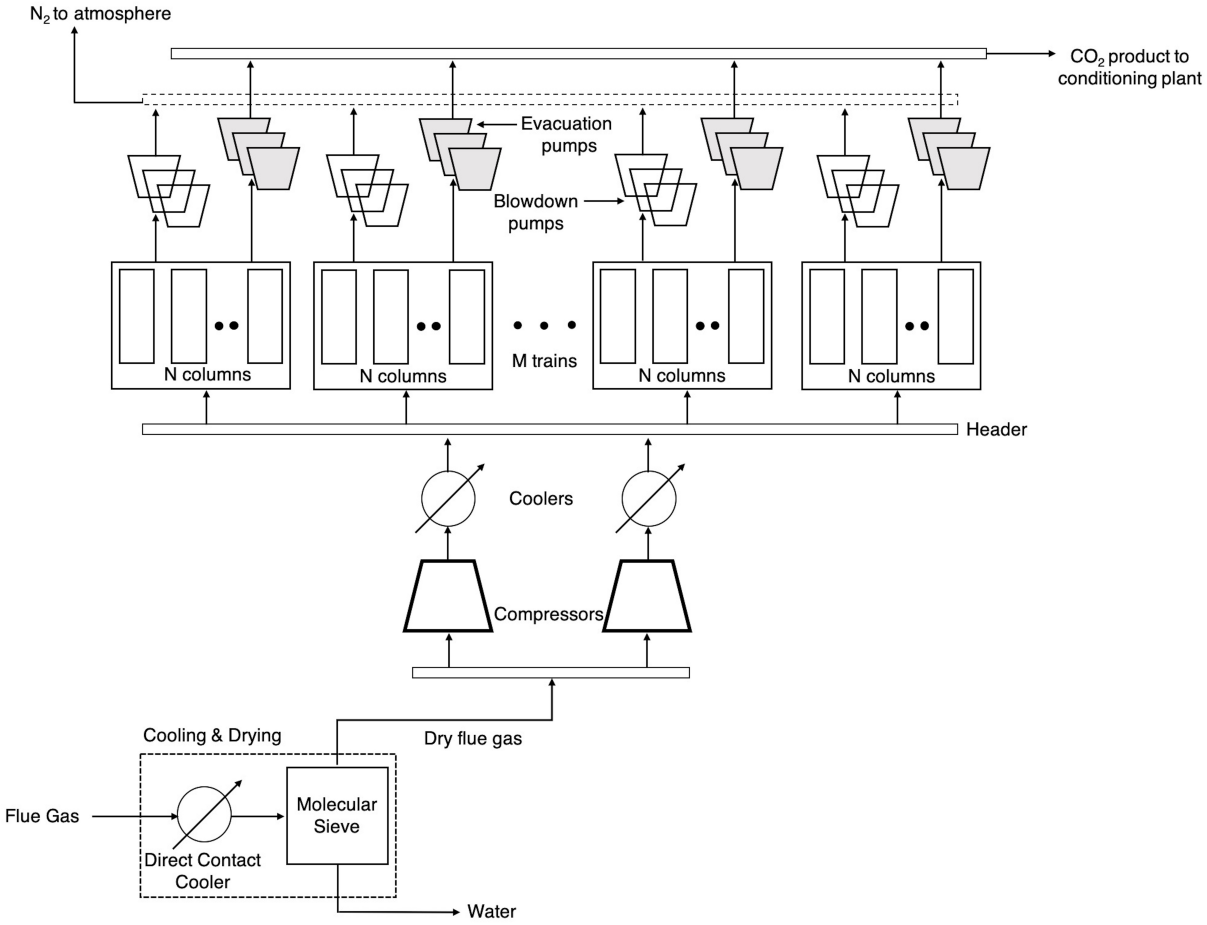

Figure 3: Process layout for CO_2 capture using vacuum swing adsorption.

3.1.2. Four Step VSA Cycle

The cycle configuration considered in this work is illustrated in Fig. 4. It is worth noting that this process is widely used in the research community as a benchmark cycle and has

This is the accepted version of an article published in Separation and Purification Technology
http://dx.doi.org/10.1016/j.seppur.2020.117832

been successfully demonstrated at a pilot-scale [16, 18, 22, 23, 24]. Naturally, more complex cycles can be synthesized resulting in better performance. However, it is anticipated that for a process of this scale, simple cycles would be preferred. The cycle consists of adsorption (ADS), co-current blowdown (BLO), counter-current evacuation (EVAC) and light product pressurisation (LPP) steps. The separation of feed mixture occurs in adsorption step at atmospheric pressure (P_{H}) where the heavy product CO_2 adsorbs in the column and N_2 leaves the column as a light product. Although adsorption step occurs at atmospheric pressure, the feed mixture needs to be compressed to a higher pressure (P_{F}) in order to overcome the pressure drop across the column. In the co-current blowdown step, the column pressure is reduced to an intermediate vacuum (P_{I}) in order to remove N_2 present in the column. The column pressure is further reduced to a low vacuum (P_{L}) in the counter-current evacuation step to collect the heavy product CO_2 at the feed end of the column. The light product from the adsorption step is used to pressurise the column back to atmospheric pressure.

This is the accepted version of an article published in Separation and Purification Technology
http://dx.doi.org/10.1016/j.seppur.2020.117832

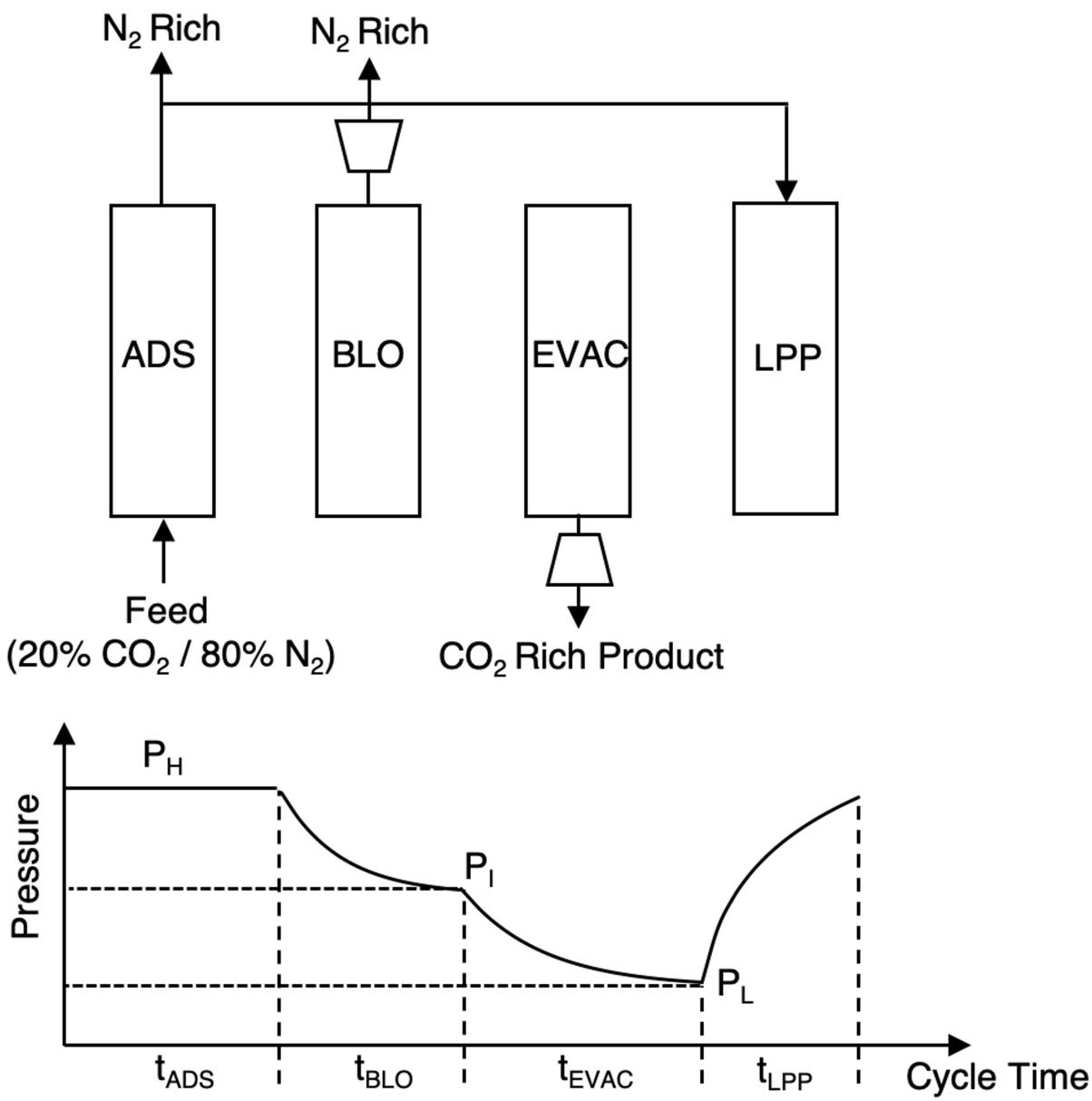

Figure 4: Four step VSA cycle schematic.

3.1.3. Adsorbent Materials

Three adsorbents were considered: Zeolite 13X [25], the current benchmark material for CO_2 capture [18, 26]; Metal-organic frameworks, UTSA-16 [27], a widely studied metal-organic framework for CO_2 capture [16, 17, 22, 28], and IISERP MOF2 [29], which showed

This is the accepted version of an article published in Separation and Purification Technology
http://dx.doi.org/10.1016/j.seppur.2020.117832

a better performance than Zeolite 13X and other MOFs in terms energy consumption and productivity in a recent screening study [30]. The adsorption equilibria for all these adsorbents were described using a competitive form dual-site Langmuir (DSL) model (for each component i):

$$q_i^* = \frac{q_{\mathrm{sb},i} b_i c_i}{1 + \sum_i b_i c_i} + \frac{q_{\mathrm{sd},i} d_i c_i}{1 + \sum_i d_i c_i} \tag{1}$$

where $q_{\mathrm{sb},i}$ and $q_{\mathrm{sd},i}$ are the saturation loadings for the two sites and, b_i and d_i are the adsorption equilibrium constants with Arrhenius temperature dependence as follows:

$$b_i = b_0 e^{\left(-\frac{\Delta U_{\mathrm{b},i}}{RT}\right)} \tag{2a}$$

$$d_i = d_0 e^{\left(-\frac{\Delta U_{\mathrm{d},i}}{RT}\right)} \tag{2b}$$

$\Delta U_{\mathrm{b},i}$ and $\Delta U_{\mathrm{d},i}$ are the internal energies of the two sites. It is worth mentioning that the extended dual-site Langmuir isotherm model in Eq. 1 explicitly takes into account the competition between CO_2 and N_2. In this work, the equal energy site (EES) form of the DSL isotherm is used [23]. In this formalism, the saturation capacity of each site is kept identical for both components and the enthalpy of adsorption for N_2 is kept identical for both sites. Experimental evidence supports this for the case of Zeolite 13X [31]. The DSL isotherm parameters for Zeolite 13X pellets were obtained based on previously performed experiments [25]. The CO_2 and N_2 isotherm parameters for UTSA-16 extrudates and IISERP MOF2 were obtained from the literature [28, 30]. Note that the IISERP MOF2 was assumed to

This is the accepted version of an article published in Separation and Purification Technology
http://dx.doi.org/10.1016/j.seppur.2020.117832

form uniform particles of 1.5 mm using a structuring agent (binder). Figure 5 shows the CO_2 and N_2 single component isotherms for all three adsorbents and related isotherm parameters are provided in Table S2 in the Supporting Information.

This is the accepted version of an article published in Separation and Purification Technology
http://dx.doi.org/10.1016/j.seppur.2020.117832

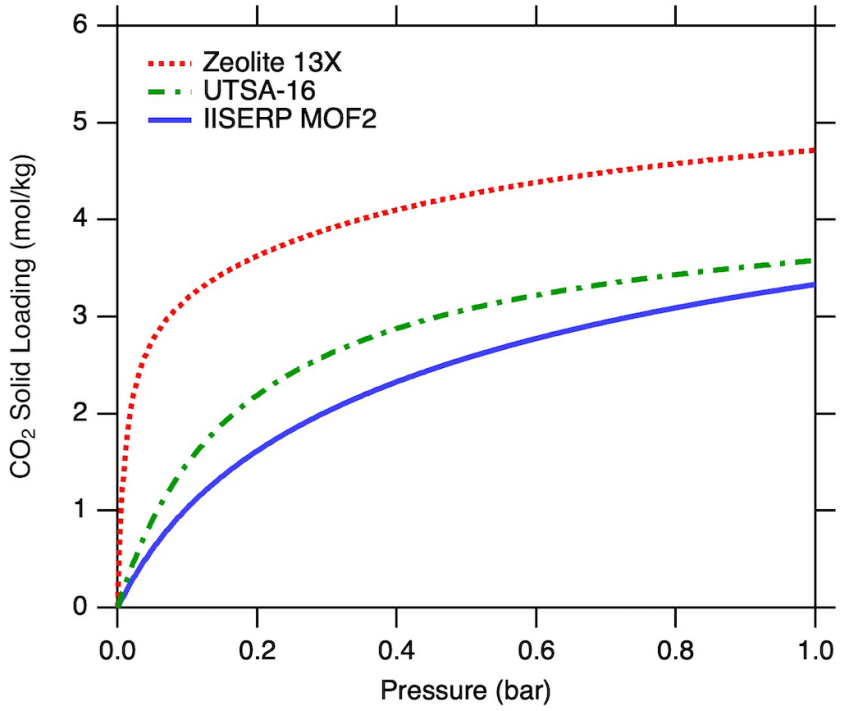

(a)

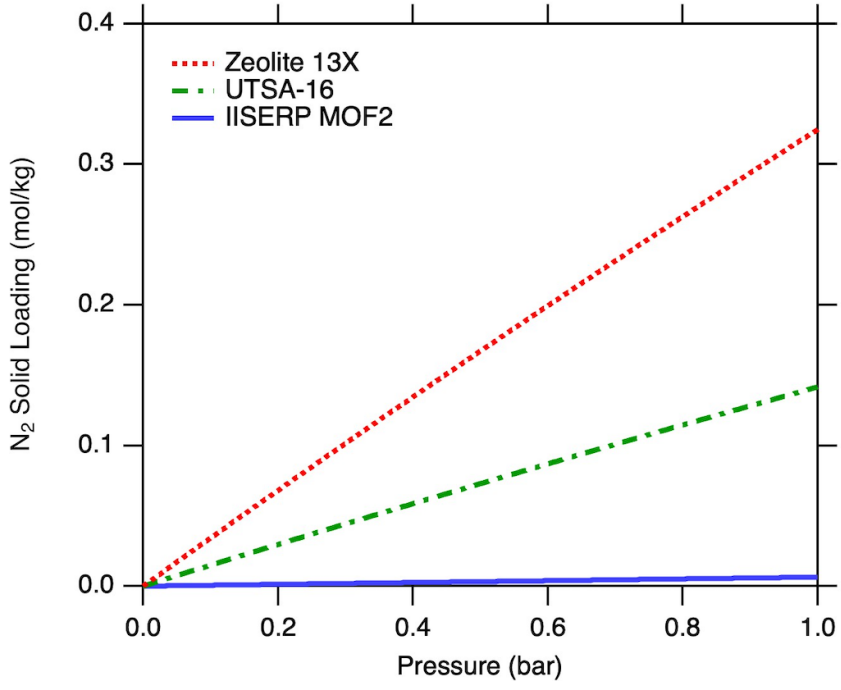

(b)

Figure 5: Single component (a) CO_2 and (b) N_2 isotherms on the three adsorbents at 298.15 K.

This is the accepted version of an article published in Separation and Purification Technology
http://dx.doi.org/10.1016/j.seppur.2020.117832

3.2. Technical Modelling

3.2.1. VSA Process Model

A non-isothermal, one-dimensional mathematical model obtained by solving mass, momentum and energy balances was used to simulate the VSA process [25]. Both lab-scale and pilot-scale experiments have been reported in the literature to validate the model [18, 31]. The model assumes that the gas behaves ideally and an axially dispersed plug flow model represents the bulk flow. No radial gradients exist for composition, pressure and temperature across the column. Adsorbent properties and bed porosity remain uniform throughout the column. There also exists an instantaneous thermal equilibrium between the gas and the solid. Linear driving force model describes the solid phase mass transfer and Ergun's equation accounts for the pressure drop across the column. Adiabatic operation, i.e. no heat transfer across the walls, remains valid given the large column sizes considered. The resulting governing equations are listed in the Supporting Information.

Appropriate boundary conditions were defined to solve each cycle step (provided in the Supporting Information). Unlike previous studies [25, 32], volumetric flow rate of vacuum pumps were assigned as boundary conditions at the exit of the column to simulate blowdown and evacuation steps instead of using predefined exponential pressure histories. This modification allows for reliable estimations of cycle times and the vacuum pump size/cost. Note that most of the vacuum pump costs are based on volumetric flow rates [16]. In addition, recent studies also show that incorporating vacuum pump volumetric flow rate based boundary conditions improve the overall accuracy of the model to predict process performance indicators [16, 33]. Therefore, volumetric flow rate of vacuum pumps were given as

This is the accepted version of an article published in Separation and Purification Technology
http://dx.doi.org/10.1016/j.seppur.2020.117832

inputs and the times of blowdown and evacuation were calculated by the model.

The partial differential equations (PDEs) were numerically solved by discretizing the spatial terms using the finite volume method with a weighted essentially non-oscillatory (WENO) scheme as a flux limiter [25]. The PDEs were discretized into 30 finite volumes and the resulting ordinary differential equations were integrated using a stiff ode solver, *ode23tb*, in MATLAB. All simulations were initialized with a feed mixture at P_{L} and were performed based on a unibed approach, i.e. a single bed undergoes all cycle steps in a sequence, a standard technique used in P/VSA simulations. The coupled cycle steps were modeled by using data buffers to store the stream information. The blowdown and evacuation steps were terminated once the column pressure reaches the desired pressure. The criterion for cyclic steady state (CSS) was when the mass balance error equal to 1% or less was observed for five consecutive cycles. Simulations were run for a large number of cycles to confirm that this criterion was adequate. If the system fails to attain the CSS criterion, simulations were performed until a maximum of 500 cycles after which it was assumed that the CSS was attained. At CSS, the model provided detailed composition, temperature and pressure profiles that were essential to calculate key performance indicators. The simulation parameters are provided in Table S4 in the Supporting Information.

3.2.2. Column Scheduling

Owing to the transient nature of VSA system, scheduling the cycle with the minimum number of columns is required to make the operation continuous. The scheduling procedure proposed by Khurana and Farooq [16] was adopted. The main considerations are sum-

marized here: (1) Continuous feed with constant throughput. (2) Separate blowdown and evacuation vacuum pumps to avoid contamination of effluents from respective steps and to maintain the modular nature of the process. (3) Coupled steps must occur simultaneously in two columns in order to avoid storage. (4) At any given time, one vacuum pump serves only one column. More details on calculating the number of columns per unit train (N), the number of vacuum pumps per unit train (N_{v}) and the number of parallel trains (M) are provided in the Supporting Information.

3.2.3. Vacuum Pumps

Vacuum pumps were assumed to deliver constant volumetric flow rates over wide vacuum ranges. Although, in practice, vacuum pump flow rates obey specific performance curves, a constant volumetric flow rate assumption allows for a more generic design framework employed herein. It is worth mentioning that the vacuum pump efficiency was considered to be dependent on the vacuum level, instead of a fixed value. Based on earlier studies, it was found that the vacuum pump performance significantly drops at deep vacuum levels (<0.1 bar) while it remains constant for moderate vacuum (>0.1 bar) [18, 19]. Although the true vacuum pump efficiency depends on the specific vacuum pump, a generalized vacuum pump efficiency function regressed based on vacuum levels between 0.01 bar and 1 bar after analyzing the several vacuum pump performance curves in a previous study [19] was used. The relation for vacuum pump efficiency is defined as follows:

$$\eta_{\mathrm{V}} = \frac{15.84P}{1 + 19.80P} \tag{3}$$

This is the accepted version of an article published in Separation and Purification Technology
http://dx.doi.org/10.1016/j.seppur.2020.117832

where P, in bar, is the suction pressure. Note that unless otherwise stated, Eq. 3 was used to quantify the vacuum pump performance in this study. The efficiency, η_V, includes that of the driver.

3.3. Cost Assessment

The cost assessment was performed on the basis of an Nth Of A Kind (NOAK) approach wherein it was assumed that the VSA technology was mature for CO_2 capture and demonstrated on a commercial scale [34]. The cost methodology for VSA technology involves estimation of both capital costs (CAPEX) and operating costs (OPEX). All costs are provided in $€_{2016}$ price levels. Costs based on older estimates than 2016 were updated using Chemical Engineering Plant Cost Index (CEPCI) and inflation.

3.3.1. Capital Costs

A bottom-up approach was adopted to estimate the capital costs and is illustrated in Fig. 6 [35]. First, the direct cost of process equipment was estimated using Aspen Process Economic Analyzer®. The direct cost of each equipment represents both equipment and installation costs. The estimation was carried out based on key design characteristics of each equipment, such as pressure, diameter, flow rate, etc. For easier implementation within the optimisation framework, cost functions were regressed for each type of equipment and were directly used to assess the direct cost of each equipment of the process. Multiple economic evaluations were performed based on a wide range of relevant key design characteristics for each equipment so that the accuracy of cost functions remain valid for different operating conditions evaluated in the optimisation (see Appendix for more details). In addition to

This is the accepted version of an article published in Separation and Purification Technology
http://dx.doi.org/10.1016/j.seppur.2020.117832

process equipment, initial adsorbent purchase, transport and installation costs were also accounted for in the total direct cost (TDC).

A process contingency factor of 15% of total direct cost without contingencies, which is in line with NETL guidelines was added to the total direct cost to calculate the total direct cost with process contingency (TDCPC) [36]. Then, indirect costs and project contingencies were added to total direct cost with process contingencies to obtain the total plant cost (TPC). Indirect costs, which include, engineering costs, consultancies, service facilities, yard improvement, building and sundries were set to 14% of TDCPC, while project contingencies were set to 20% of TDCPC in accordance with NETL guidelines [36]. Finally, the owner costs and interest over construction are added to the TPC to calculate the total capital requirement (TCR). The owner costs are considered to represent 7% of TDCPC [37] and the interest over construction are calculated assuming that the construction costs are shared over a three-year construction period following a 40/30/30 allocation.

Due to its specificity, it is worth noting that the direct cost of each adsorbent was estimated differently than presented above. While the cost of an adsorbent is key for the design and evaluation of adsorption-based CO_2 capture processes, estimating the cost of an adsorbent can be challenging in practice, especially if the material has not been commercialized. Amongst the adsorbents considered in this work, Zeolite 13X is the only one that has been deployed industrially and its purchase cost was estimated to 1500 € per tonne [17]. However, UTSA-16 and IISERP MOF2, and more generally MOFs, are still in early development stages with no information on large-scale production and thus with no well-established cost. While the cost of synthesizing MOFs are currently very high, as these

are mainly grams-level quantities synthesized at the lab-scale. The potential for scale-up through application like CCS would be expected to significantly reduce the production cost for MOFs reaching the commercial stage [17]. Under such circumstances, the cost of raw materials could be expected to represent a similar level of the MOF cost than the synthesis cost. Therefore, in this work, the purchase cost of MOFs were assumed to be twice the cost of metals used to synthesize them as the metals of these MOFs can be expected to be the main material cost as they typically are orders of magnitude more expensive than the organic components. For both UTSA-16 and IISERP MOF2, the costs of their underlying metals, cobalt and nickel respectively, were determined based on bulk prices per tonne from the United States Geological Survey website [38]. Based on the aforementioned assumptions, the potential purchase costs at larger production scale was estimated in terms of relative metal content and calculated to be 16640 and 4440 € per tonne for UTSA-16 and IISERP MOF2, respectively. Finally, in addition to adsorbent purchase costs, transport and installation costs associated with adsorbents was set to 1500 € per tonne for all adsorbents to reach the adsorbent direct cost, irrespective of the adsorbent considered. For commercial adsorbents, transport and installation costs are usually in the same range as the adsorbent purchase cost. This was set as the cost of Zeolite 13X.

Figure 6: Illustration of the adopted bottom-up approach for calculating investment costs [35].

3.3.2. Operating Costs

Operating costs consists of fixed and variable operating costs. The annual fixed operating costs include maintenance, labor, insurance and administrative costs. The annual maintenance cost was calculated as 2.5% of TPC of which the maintenance labor cost accounts for 40%. The annual insurance and location taxes which include overhead and miscellaneous regulatory fees were set to 2% of TPC. The labor costs were calculated based on the assumption that the CO_2 capture unit requires 5 operators (5 shift pattern with 1 operator per shift as adsorption processes are highly automated) with an annual salary of 60000 € per person. Administrative costs were set to 30% of the operating and maintenance labor cost.

One important operating cost can be that associated with adsorbent replacement over time due thermal or mechanical degradation. While some commercial adsorbents can be operated up to 20 years without replacement by careful design and proper control strategies [39], the lifetime of MOFs is still unknown. Hence, to be conservative, the replacement time for all adsorbents was set to 5 years [15, 17]. The adsorbent replacement costs, which include purchase, transport and installation costs, are incurred every 5 years after the start of the plant to replace the adsorbent.

Variable operating costs include utilities like electricity and cooling water, as well as adsorbent replacement. The annual cost for utilities was calculated based on estimated consumption from process simulations. The unit costs of utilities are provided in Table 2.

Table 2: Unit costs of utilities

Utility	**Price**
Electricity (€ $\cdot MW^{-1}h^{-1}$)	58.1 [41]
Specific Direct Emissions (kg CO_2 $\cdot MW^{-1}h^{-1}$)	38 [21]
Cooling Water (€ $\cdot m^{-3}$)	0.039 [41]

3.4. Key Performance Indicators

3.4.1. Key Technical Performance Indicators

The CO_2 purity, CO_2 recovery, overall power consumption, specific energy consumption and productivity were defined as follows:

$$CO_2 \text{ Purity } (\%) = \frac{\text{total moles of } CO_2 \text{ in the product step}}{\text{total moles of gas in the product step}} \cdot 100 \tag{4a}$$

$$CO_2 \text{ Recovery } (\%) = \frac{\text{total moles of } CO_2 \text{ in the product step}}{\text{total moles of } CO_2 \text{ in the feed step}} \cdot 100 \tag{4b}$$

Overall power consumption (P_{el}) was defined as the product of the power consumption in each unit train and the number of parallel trains (M) [16].

$$\text{Overall Power Consumption, } P_{\text{el}} \ (MW_e) = M \cdot \left(N_{\text{ADS}} \cdot \frac{E_{\text{ADS}}(J_e)}{t_{\text{ADS}}(s) \cdot 10^6} + N_{\text{BLO}} \cdot \frac{E_{\text{BLO}}(J_e)}{t_{\text{BLO}}(s) \cdot 10^6} + N_{\text{EVAC}} \cdot \frac{E_{\text{EVAC}}(J_e)}{t_{\text{EVAC}}(s) \cdot 10^6} \right) \tag{4c}$$

The power consumption in the unit train was calculated by averaging the energy consumed in each step of the VSA cycle over the duration of each step. In other words, it represents the integral average of the power demand in each step of the VSA cycle. In Eq. 4c, N_{ADS}=1

This is the accepted version of an article published in Separation and Purification Technology
http://dx.doi.org/10.1016/j.seppur.2020.117832

in the adsorption step; N_{BLO} represents the number of dedicated vacuum pumps per unit train for the blowdown step and; N_{EVAC} represents the number of dedicated vacuum pumps per unit train for the evacuation step.

It is worth noting that the power demand calculated based on Eq. 4c assumes that all movers operate continuously throughout the cycle duration. This always holds true for the compressor in the adsorption step due to continuous feed consideration in the column scheduling. On the contrary, the number of blowdown and evacuation vacuum pumps that are active will be less than or equal to N_{BLO} and N_{EVAC}, respectively, at any given time of the cycle duration. To elaborate, consider, for instance, evacuation vacuum pumps. There would a certain portion of the cycle schedule which operates with exactly N_{EVAC} vacuum pumps, yet, there also exists other portions of the cycle schedule which would operate with fewer than N_{EVAC} vacuum pumps. Under such circumstances, the power demand from the evacuation step will be based on vacuum pumps, less than N_{EVAC}, operating actively to implement the cycle. Moreover, there will be no power consumption from the remaining evacuation vacuum pumps that are inactive. Accounting for such variations in the power consumption for blowdown and evacuation steps may provide a slightly lower estimate for the overall power consumption, albeit, the assumption that all vacuum pumps operate continuously performing same work throughout the cycle duration will conservatively estimate the overall power consumption and will also be in compliance with the realistic operation. In addition

This is the accepted version of an article published in Separation and Purification Technology
http://dx.doi.org/10.1016/j.seppur.2020.117832

to overall power consumption, specific energy consumption was also defined as follows:

$$\text{Specific energy consumption (kWh}_\text{e}\ {t_{CO_2}}^{-1}) = \frac{\text{Overall Power Consumption (kW}_\text{e}) \cdot \text{Operating hours (h year}^{-1})}{\text{CO}_2\text{ captured (tonne year}^{-1})} \quad (4d)$$

Productivity was defined by considering the entire VSA capture unit as shown below:

$$\text{Productivity, } Pr\ (\text{mol m}^{-3}\ \text{s}^{-1}) = \frac{\text{CO}_2\text{ capture rate for the plant (mol s}^{-1})}{\text{total adsorbent volume used in the plant (m}^3)} \quad (4e)$$

Note that CO_2 capture rate (mol s^{-1}) was defined as the product of CO_2 recovery (-) and CO_2 molar flow rate in the flue gas (mol s^{-1}).

3.4.2. Key Economic Performance Indicators

The CO_2 avoided cost was considered as the key economic performance indicator to compare the cost performance of adsorption-based CO_2 capture technology with MEA-based CCS. It approximates the average discounted CO_2 tax or quota over the duration of the project that would be required as income to match the net present value of additional capital and operating costs due to CCS infrastructure [34]. Since the implementation of CCS does not impact the hydrogen production of the plant (key product), CO_2 avoided cost was calculated through a net present value approach [40]. The CO_2 avoided cost, in €/$t_{CO_2\text{ avoided}}$ (where $t_{CO_2\text{ avoided}}$ is metric tonnes of CO_2 avoided) is defined as shown below:

$$\text{CO}_2\text{ Avoided Cost} = \frac{\text{Net Present Value of CCS implementation cost}}{\text{Net Present Value of CO}_2\text{ avoided}} \quad (5)$$

This is the accepted version of an article published in Separation and Purification Technology
http://dx.doi.org/10.1016/j.seppur.2020.117832

Or more specifically,

$$\text{CO}_2 \text{ Avoided Cost} = \frac{\sum_i \frac{\text{TCR}_{\text{CCS implementation }(i)} + \text{Annual OPEX }_{\text{CCS implementation }(i)}}{(1+d)^i}}{\sum_i \frac{\text{Annual amount of CO}_2 \text{ emissions avoided by CCS implementation }(i)}{(1+d)^i}} \quad (6)$$

where i is the year index (-).

The amount of CO_2 emissions avoided by CCS implementation was defined as the difference of annual amount of CO_2 captured by CCS implementation and direct emissions due to heat and electricity associated with CCS implementation. Direct emissions due to electricity can be calculated using the following equation:

$$\text{Direct emissions} = e_{\text{el}} \cdot P_{\text{el}} \text{ (MW}_\text{e}\text{)} \cdot \text{Operating hours (h year}^{-1}\text{)} \quad (7)$$

where e_{el} is the specific CO_2 emissions associated with each unit of electric power consumed (kg CO_2 MW_e^{-1} h^{-1}). By taking into account direct emissions, the equivalent CO_2 avoided indicates the true overall reduction in CO_2 emissions of the SMR plant when adsorption capture technology is implemented and allows for a fair comparison with different capture technologies [41]. The financial parameters used to calculated CO_2 avoided cost are listed in Table 3.

The CO_2 capture cost was also considered to optimise the VSA process and to compare the cost performances of different adsorbents. The CO_2 capture cost, in $€/t_{CO_2 \text{ avoided}}$ is

defined as follows:

$$\text{CO}_2 \text{ Capture Cost} = \frac{\sum_i \frac{\text{TCR}_{\text{VSA capture plant }(i)} + \text{Annual OPEX }_{\text{VSA capture plant }(i)}}{(1+d)^i}}{\sum_i \frac{\text{Annual amount of CO}_2 \text{ emissions avoided by VSA capture plant }(i)}{(1+d)^i}} \quad (8)$$

It is worth noting that the CO_2 capture cost corresponds to the CO_2 avoided cost in Eq. 6 without the cost of flue gas cooling and drying, CO_2 conditioning, CO_2 transport and storage, since these costs are expected to be identical for all adsorbents.

Table 3: Financial parameters used for calculating CO_2 avoided and capture costs [21].

Parameter	**Value**
Economic lifetime (years)	25
Capacity factor (%)	91.3
CO_2 capture plant construction time (years)	3
Allocation of CO_2 capture construction costs by year (%)	40/30/30
Discount Rate (%)	8

3.5. Techno-economic Optimisation Model

The VSA process design was approached as an integrated techno-economic optimisation framework by identifying optimal design and operating variables of the process as illustrated in Fig. 2. The optimisation methodology integrates process and material aspects together with cost models in order to minimize CO_2 capture cost while ensuring a minimum of 90% CO_2 recovery and 95% CO_2 purity. The set of variables include, adsorption step duration (t_{ADS}), blowdown step interstitial velocity (v_{B}), evacuation step interstitial velocity (v_{E}), intermediate vacuum (P_{I}), evacuation vacuum (P_{L}), interstitial feed velocity (v_0) and column length (L).

This is the accepted version of an article published in Separation and Purification Technology
http://dx.doi.org/10.1016/j.seppur.2020.117832

The choice of design and operating variables depend on the VSA cycle and the adsorbent used. For the four step VSA cycle considered, t_{ADS} and v_0 can be tuned in the adsorption step to control the feed flow rate and also the CO_2 front propagation along the column. Since this step operates at atmospheric pressure, the feed pressure can be calculated based on Ergun's equation. For blowdown and evacuation steps, vacuum levels, P_{I} and P_{L}, respectively are variables. In addition, volumetric flow rates of blowdown (S_{B}) and evacuation vacuum pumps (S_{E}) can be also varied for respective steps. To this end, S_{B} and S_{E} were implicitly varied in terms of the interstitial velocities, v_{B} and v_{E}, respectively. This was done to provide an appropriate vacuum pump sizing range for the columns and also, a limit of 20000 $\mathrm{m^3\ h^{-1}}$ was implicitly enforced on the maximum vacuum pump size. It is worth mentioning that the durations of blowdown and evacuation steps are calculated by the model based on S_{B} and S_{E}, respectively. Finally, the duration of light product pressurisation depends on t_{ADS} and is not considered as the variable in the optimisation. Owing to the scale-up design, the column length, L was considered as a variable. As both column length and column diameter can be varied simultaneously, the column length-to-diameter (L/D) ratio was, however, kept constant in the optimisations. The lower and upper bounds defined for the variables are provided in Table 4.

Table 4: Decision variable bounds used in the optimisation.

	t_{ADS} (s)	v_{B} ($\mathrm{m\ s^{-1}}$)	v_{E} ($\mathrm{m\ s^{-1}}$)	P_{I} (bar)	P_{L} (bar)	v_0 ($\mathrm{m\ s^{-1}}$)	L (m)
Lower bound	50	0.2	0.2	P_{L} + 0.01	0.01	0.1	3
Upper bound	400	3	3	0.9	0.05	1.2	9

This is the accepted version of an article published in Separation and Purification Technology
http://dx.doi.org/10.1016/j.seppur.2020.117832

The constrained optimisation problem was transformed into an unconstrained problem by adding penalty terms to the objective function which impose high costs when constraints are violated and was solved using a non-dominated sorting genetic algorithm II (NSGA-II), a global search method that converges towards optimal solution(s) by mimicking the process of evolution. In other words, the algorithm initializes a unique set of decision variables chosen within the bounds using Latin hypercube sampling and evaluates for objective functional values based on integrated VSA process and cost models. This set of decision variables represents a generation. NSGA-II improves the objective functional values by utilizing some additional operations such as mutation and crossover over multiple generations. Global optimisation and parallelization toolboxes in MATLAB 2018b were employed to implement the optimisation. The population size was set to 24 times the number of variables and the stopping criterion for the optimisation was 50 generations.

4. Results and Discussion

4.1. Design and cost of the optimal adsorption-based CO_2 capture processes

The VSA process for each adsorbent was optimised for the minimum CO_2 capture cost with requirements of 95% CO_2 purity and 90% CO_2 recovery. Table 5 shows the process variables optimised for the minimum capture cost together with technical performances and other design details of the VSA process. In these optimisations, for the base-case scenario, the length-to-diameter ratio of adsorption columns was fixed at 3. For the cycle considered, all three adsorbents met the purity-recovery requirements by demanding deep vacuum, i.e. ≤ 0.036 bar, to evacuate the CO_2 product out of the column. It can be observed that the

This is the accepted version of an article published in Separation and Purification Technology
http://dx.doi.org/10.1016/j.seppur.2020.117832

size requirement of the vacuum pump depends on the intermediate vacuum (P_{I}) and low vacuum (P_{L}) levels. Owing to the larger swing between P_{I}=0.31 bar and P_{L}=0.036 bar for IISERP MOF2 in the evacuation step, the optimiser chose very large evacuation vacuum pump (>16000 m^3 h^{-1}) to avoid long durations of the evacuation step, thereby, limiting the number of columns and evacuation vacuum pumps needed for scheduling. For Zeolite 13X and UTSA-16, vacuum pumps of capacity $\approx$ 8500-13000 m^3 h^{-1} seemed to be sufficient to reduce the vacuum levels from P_{I} of 0.11 bar to P_{L} of 0.022 and 0.026 bar, respectively, in the evacuation steps. Although larger vacuum pumps might perhaps be used for these cases, it can be inferred that the optimiser found the trade-off between the size requirement and the vacuum pump power consumption as the optimal flow rates have not approached the limits of the specified ranges in the optimisation. The non-linear nature of the CO_2 isotherms on Zeolite 13X and UTSA-16 compared to linear CO_2 isotherm on IISERP MOF2 could have also contributed to this choice. Similar observations can be made for optimiser's choice of blowdown vacuum pumps based on intermediate vacuum (P_{I}). As can be seen from the table, longer columns (>5 m) are needed to reduce the total number of columns. Also, interstitial feed velocities for all cases are either close to or at the upper bound in order to facilitate the reduction in the number of parallel trains. Due to long columns and high interstitial velocities, the flue gas is compressed (>1.5 bar) to overcome the pressure drops across the column. Though the upper limit for the column length was kept at 9 m, power losses due to large pressure drops and very long evacuation times might have discouraged the optimiser to choose column lengths in close proximity to the upper limit.

This is the accepted version of an article published in Separation and Purification Technology
http://dx.doi.org/10.1016/j.seppur.2020.117832

Table 5: Process performances of the four step adsorption cycle for different materials that were optimised for the minimum capture cost.

	Base Case		
Adsorbent	Zeolite 13X	UTSA-16	IISERP MOF2
Vacuum pump efficiency	Variable	Variable	Variable
Objective function	Min. Cost	Min. Cost	Min. Cost
Operating Conditions			
Adsorption time (s)	212	159	118
Blowdown pump flow rate ($m^3\ h^{-1}$)	7784	6086	5434
Evacuation pump flow rate ($m^3\ h^{-1}$)	12682	8631	16341
Maximum feed pressure (bar)	1.92	1.53	2.03
Intermediate pressure (bar)	0.11	0.11	0.31
Low pressure (bar)	0.022	0.026	0.036
Feed velocity ($m\ s^{-1}$)	1.14	1.20	1.20
Column Length (m)	8.0	5.4	8.8
Length-to-diameter ratio (-)	3.0	3.0	3.0
Train Configuration			
Number of columns per train (-)	7	4	4
Number of blowdown pumps per train (-)	1	1	1
Number of evacuation pumps per train(-)	5	3	3
Number of parallel trains (-)	42	97	29
Process Performance			
Purity (%)	94.9	95.0	95.1
Recovery (%)	91.0	90.0	91.4
Productivity ($mol\ m^{-3}\ s^{-1}$)	1.89	4.45	3.61
Compressor power (MW_e)	12.00	7.91	14.10
Blowdown power (MW_e)	4.39	8.78	1.24
Evacuation power (MW_e)	41.77	39.22	22.45
Overall power consumption (MW_e)	58.15	55.90	37.79
Specific energy consumption (kWh_e/t_{CO_2})	307.86	299.53	199.33

Based on the optimised process variables, the VSA cycle schedule is illustrated in Fig. S3 in the Supporting Information. Idle times are included wherever deemed necessary. To treat the entire dry flue gas in a continuous manner, a total of 42 parallel trains with seven columns per train, 97 parallel trains with four columns per train and 29 parallel trains with four columns per train are necessary for Zeolite 13X, UTSA-16 and IISERP MOF2 cases, respectively. Clearly, the MOFs achieved higher productivities, i.e. less adsorbent volume as compared to Zeolite 13X. For this scale of capture unit, the total power consumption

This is the accepted version of an article published in Separation and Purification Technology
http://dx.doi.org/10.1016/j.seppur.2020.117832

based on compressors, all blowdown and evacuation vacuum pumps pertaining to all parallel trains is shown in Table 5. As expected, evacuation step consumes most of the total power. UTSA-16 and Zeolite 13X require high power consumption while IISERP MOF2 has the lowest power consumption. This observation is consistent with previous studies have shown that this can be explained by the low N_2 affinity of an adsorbent [30, 42].

The cost breakdowns for all adsorbents corresponding to the lowest capture cost are provided in Table 6. In addition, other costs pertaining to flue gas pre-treatment (i.e. cooling and drying), CO_2 conditioning, transport and storage costs are also reported for all adsorbents. It is worth noting that all cost breakdowns are reported in €/$t_{CO2,\ avoided}$. Since the overall framework remains the same for all adsorbents, capture costs are compared to assess the performance of each of the adsorbents. As can be seen from the table, IISERP MOF2 is the best performing adsorbent for the VSA process considered. For IISERP MOF2, the capital costs constitute about 36% where the contributions from columns (≈6%), compressors (≈5%) and vacuum pumps (≈6%) have similar magnitudes. On the other hand, the operating costs for IISERP MOF2 sum up to 64%, including both fixed and variable operating costs. As expected, the major contribution arises from the power consumption (≈38% of the capture cost). It is worth noting that the fixed operating costs are dependent on the total capital requirement. UTSA-16 has the highest capture cost as compared to the other two adsorbents. This is primarily due to exorbitant adsorbent costs. Adsorbent costs constitute 20% of the total capture costs. This is strikingly high compared to IISERP MOF2 (≈13%) and Zeolite 13X (9%) due to the presence of expensive metal source cobalt. The high adsorbent costs prohibited the optimiser to increase the column volume, thereby increasing

This is the accepted version of an article published in Separation and Purification Technology
http://dx.doi.org/10.1016/j.seppur.2020.117832

the number of parallel trains. This observation was corroborated by a case study in a later section where the influence of MOF prices on the capture cost was considered. In addition, high power consumption also remains a significant contributor. Zeolite 13X requires more number of columns per unit train as compared to MOFs because of the non-linear nature of the CO_2 isotherm. For this reason, huge capital is needed while relatively higher N_2 affinity increased the electricity costs.

This is the accepted version of an article published in Separation and Purification Technology
http://dx.doi.org/10.1016/j.seppur.2020.117832

Table 6: CO_2 avoided costs breakdown of the four step adsorption cycle for different materials that were optimised for the minimum capture cost. A value of 0.0 indicates that the contribution was less than 0.1 €/$t_{CO_2,\ avoided}$.

		Base Case	
Adsorbent	Zeolite 13X	UTSA-16	IISERP MOF2
Vacuum pump efficiency	Variable	Variable	Variable
Objective function	Min. Cost	Min. Cost	Min. Cost
	€/$t_{CO_2,\ avoided}$	€/$t_{CO_2,\ avoided}$	€/$t_{CO_2,\ avoided}$
Cooling & Drying	**2.8**	**2.8**	**2.8**
CAPEX Cooling & Drying	2.2	2.2	2.2
Fixed OPEX Cooling & Drying	0.3	0.3	0.3
Variable OPEX Cooling & Drying	0.3	0.3	0.3
VSA Capture	**48.6**	**62.1**	**30.8**
CAPEX	18.6	25.1	11.1
Total Direct Cost	11.5	15.5	6.9
Column Cost	3.8	3.6	1.7
Compressor Cost	1.5	1.5	1.5
Vacuum Pump Cost	3.8	4.8	1.9
Heat Exchanger Cost	0.0	0.0	0.0
Valves Cost	0.4	0.5	0.1
Initial Adsorbent Cost	1.9	5.1	1.6
Process Contingency	1.7	2.3	1.0
Indirect Cost	1.9	2.5	1.1
Project Contingency	2.6	3.6	1.6
Owner Cost	0.9	1.2	0.5
OPEX	30.0	37.0	19.7
Fixed OPEX	9.0	12.1	5.5
Electricity Cost	18.1	17.6	11.7
Adsorbent Cost	2.7	7.2	2.3
Cooling Water Cost	0.2	0.1	0.2
CO_2 Conditioning	**8.7**	**8.8**	**8.7**
CAPEX Conditioning	2.4	2.4	2.4
Fixed OPEX Conditioning	0.4	0.4	0.4
Electricity Cost Conditioning	5.9	6.0	5.9
CO_2 Pipeline	**12.2**	**12.4**	**12.2**
CAPEX Pipeline	10.9	11.0	10.8
Fixed OPEX Pipeline	1.3	1.4	1.4
CO_2 Storage	**18.6**	**18.8**	**18.5**
CAPEX Storage	15.2	15.3	15.1
Fixed OPEX Storage	2.5	2.5	2.5
Variable OPEX Storage	0.9	0.9	0.9
CO_2 Avoided Cost	**90.9**	**104.9**	**73.0**

4.2. Importance of process design objectives

The most common choice of process design objectives while designing or comparing optimal VSA processes for post-combustion CO_2 capture has been either energy consumption

This is the accepted version of an article published in Separation and Purification Technology
http://dx.doi.org/10.1016/j.seppur.2020.117832

linked to the VSA or productivity or both [19, 22, 24, 25]. Besides, few studies also considered lowering total costs in their process designs [13, 14, 15, 16]. Generally, the rationale behind the choice of design objectives is that the energy consumption approximates the operating costs and productivity gives a rough estimation of capital costs as well as operating costs related to the adsorbent. Although this might hold true when the adsorbents under consideration have similar costs and designing a single unit VSA train. The CO_2 capture problem, on the other hand, requires several number of VSA trains in order to treat the entire flue gas. Thus, choosing an appropriate design objective remains critical, especially when optimising or comparing VSA with different CO_2 capture technologies. To this end, different process design objectives were examined through an optimisation study to comprehend the influence of each design objective towards achieving lower cost of CO_2 capture. Three optimisation problems that are commonly used in the literature were considered in addition to the minimization of CO_2 capture cost and are described below.

- Problem 1: Minimization of overall power consumption
- Problem 2: Maximization of productivity
- Problem 3: Minimization of overall power consumption and maximization of productivity

Optimisation runs were performed for each of these cases based on both IISERP MOF2 and Zeolite 13X as adsorbents. The reason for choosing IISERP MOF2 and Zeolite 13X for the case study is that the IISERP MOF2 provides a representative case for VSA because of

This is the accepted version of an article published in Separation and Purification Technology
http://dx.doi.org/10.1016/j.seppur.2020.117832

its superior performance as compared to other adsorbents and Zeolite 13X represents the case for commercial adsorbents. The base results pertaining to the minimization of the capture cost are shown in Table 6. Note that unless otherwise stated, the optimal techno-economic performance obtained from the minimization of capture cost is referred herein as the minimum capture cost case. After unique optimisation runs, the techno-economic performances corresponding to the minimum overall power consumption and maximum productivity were evaluated and reported in Table 7 as Case I and Case II, respectively. Consider, for instance, the minimization of overall power consumption. For IISERP MOF2, the lowest power consumption obtained was 25.56 MW_e, notably, a 34% difference when compared to the power consumption linked to the minimum capture cost case. The optimiser selected smaller columns and small-sized vacuum pumps in order to minimize the pressure drop losses and power consumption associated with the vacuum pumps. However, the capture cost of the four-step adsorption cycle optimised based on the minimum overall power consumption was almost 184% higher than that of the reference minimum capture cost. This strikingly high capture cost comes from the enormous capital expenditure and related footprint required to treat the entire flue gas based on smaller columns. The total number of columns required was 1593, owing to which the column cost increased by ≈760% as compared to the minimum capture cost case. Considering the scheduling, the total number of vacuum pumps needed has also increased from 116 to 1416. While the total power consumed by all of these vacuum pumps is minimal, the capital expenditure related to these vacuum pumps has increased by ≈3.5× that of the minimum capture cost case. In addition, adsorbent, valves and fixed operating costs associated to the capital expenditure have also increased. On the

This is the accepted version of an article published in Separation and Purification Technology
http://dx.doi.org/10.1016/j.seppur.2020.117832

other hand, the electricity costs are almost 32% lower compared to the minimum capture cost case. Similar observations can be made for Zeolite 13X. The capture cost related to the minimum overall power consumption is 244% more than the minimum capture cost. The power consumption lowered to ≈35 MW_e, i.e. a difference of ≈23 MW_e, at the expense of 432% more capital expenditure compared to the minimum capture cost case. Owing to process behaviour of achieving lower overall power consumption at lower productivity, the productivity obtained in these cases will be lower than the minimum capture cost scenario. This clearly explains that the process design must not solely focus on minimization of overall power consumption, but must also take into account the associated capital and operating costs.

Case II in Table 7 shows techno-economic performances corresponding to the maximum productivity. Again, the capture cost related to the maximum productivity remains 124% higher than the minimum capture cost for IISERP MOF2. Interestingly, the optimised column length has reached the lower bound in the optimisation. This is because the optimiser selected the lowest possible adsorbent volume to increase the productivity of the process. Further, the cycle duration has also shortened, thereby facilitating the increase in productivity by reducing the number of columns per train. The overall power consumption rose to ≈53 MW_e as compared to ≈38 MW_e in the minimum capture cost case, resulting in ≈44% more electricity costs. For Zeolite 13X, capture cost corresponding to the maximum productivity was ≈124% higher than the minimum capture cost.

This is the accepted version of an article published in Separation and Purification Technology
http://dx.doi.org/10.1016/j.seppur.2020.117832

Table 7: Techno-economic performances for case studies relating to the choice of objective function, i.e., overall power consumption (P_{el}) and productivity (Pr). Note that * indicates the change made with respect to reference cases in Tables 5 and 6.

	Case I	**Case I**	**Case II**	**Case II**
Adsorbent	Zeolite 13X	IISERP MOF2	Zeolite 13X	IISERP MOF2
Vacuum pump efficiency	Variable	Variable	Variable	Variable
Objective function	Min. P_{el}*	Min. P_{el}*	Max. Pr*	Max. Pr*
Operating Conditions				
Adsorption time (s)	265	188	213	107
Blowdown pump flow rate ($m^3\ h^{-1}$)	355	707	3195	3040
Evacuation pump flow rate ($m^3\ h^{-1}$)	439	1045	2241	2584
Maximum feed pressure (bar)	1.30	1.24	1.17	1.22
Intermediate pressure (bar)	0.22	0.35	0.10	0.35
Low pressure (bar)	0.023	0.032	0.014	0.018
Feed velocity ($m\ s^{-1}$)	1.08	0.79	0.88	1.10
Column Length (m)	3.7	5.4	3.0	3.0
Length-to-diameter ratio (-)	3.0	3.0	3.0	3.0
Train Configuration				
Number of columns per train (-)	18	9	4	3
Blowdown pumps per train (-)	1	1	1	1
Evacuation pumps per train (-)	16	7	3	2
Number of parallel trains (-)	263	177	533	420
Process Performance				
Purity (%)	95.0	94.9	95.0	95.0
Recovery (%)	90.2	90.0	90.8	89.9
Productivity ($mol\ m^{-3}\ s^{-1}$)	1.13	1.10	4.68	8.01
Compressor power (MW_e)	4.63	3.86	2.63	3.39
Blowdown power (MW_e)	1.19	1.33	27.12	15.85
Evacuation power (MW_e)	28.77	20.37	57.29	34.20
Overall power consumption (MW_e)	34.59	25.56	87.04	53.44
Specific energy consumption (kWh_e/t_{CO_2})	184.93	136.98	461.98	286.52
Cost Performance				
CAPEX (€/$t_{CO_2,\ avoided}$)	99.0	48.7	54.7	34.5
Total Direct Cost (€/$t_{CO_2,\ avoided}$)	61.0	30.1	33.7	21.3
Column Cost (€/$t_{CO_2,\ avoided}$)	34.4	14.6	14.1	8.4
Compressor Cost (€/$t_{CO_2,\ avoided}$)	1.5	1.5	1.5	1.5
Vacuum Pump Cost (€/$t_{CO_2,\ avoided}$)	16.1	6.7	14.6	9.1
Heat Exchanger Cost (€/$t_{CO_2,\ avoided}$)	0.0	0.0	0.0	0.0
Valves Cost (€/$t_{CO_2,\ avoided}$)	5.8	2.0	2.6	1.6
Initial Adsorbent Cost (€/$t_{CO_2,\ avoided}$)	3.2	5.3	0.8	0.7
Process Contingency (€/$t_{CO_2,\ avoided}$)	9.2	4.5	5.1	3.2
Indirect Cost (€/$t_{CO_2,\ avoided}$)	9.8	4.8	5.4	3.4
Project Contingency (€/$t_{CO_2,\ avoided}$)	14.0	6.9	7.8	4.9
Owner Cost (€/$t_{CO_2,\ avoided}$)	4.9	2.4	2.7	1.7
OPEX (€/$t_{CO_2,\ avoided}$)	62.2	38.8	54.4	34.4
Fixed OPEX (€/$t_{CO_2,\ avoided}$)	46.8	23.2	25.9	16.5
Electricity Cost (€/$t_{CO_2,\ avoided}$)	10.8	8.0	27.3	16.8
Adsorbent Cost (€/$t_{CO_2,\ avoided}$)	4.5	7.5	1.1	1.0
Cooling Water Cost (€/$t_{CO_2,\ avoided}$)	0.1	0.1	0.1	0.1
VSA Capture Cost (€/$t_{CO_2,\ avoided}$)	**161.2**	**87.5**	**109.1**	**68.9**

This is the accepted version of an article published in Separation and Purification Technology
http://dx.doi.org/10.1016/j.seppur.2020.117832

Figure 7(a) shows the Pareto solutions obtained from the multi-objective optimisation where overall power consumption was minimized simultaneously by maximizing the productivity. For comparison, results obtained from minimization of CO_2 capture cost, minimization of overall power consumption, i.e. Case I, and maximization of productivity (Case II) are also shown. Generally, the Pareto solutions represent the best trade off between the overall power consumption and the productivity and provide approximations for the best cost performances. Any point below the Pareto curve remains infeasible while any point that lies above the curve corresponds to suboptimal point. As can be observed from the figure, the minimum capture cost lies in the suboptimal region of the Pareto plot, indicating that the multi-objective optimisation formulations involving productivity and energy consumption do not provide complete information about costs. This can be clearly seen in Fig. 7(b). It is therefore clear that the best objective for optimising VSA processes related to CO_2 capture problem is the capture cost [14].

This is the accepted version of an article published in Separation and Purification Technology
http://dx.doi.org/10.1016/j.seppur.2020.117832

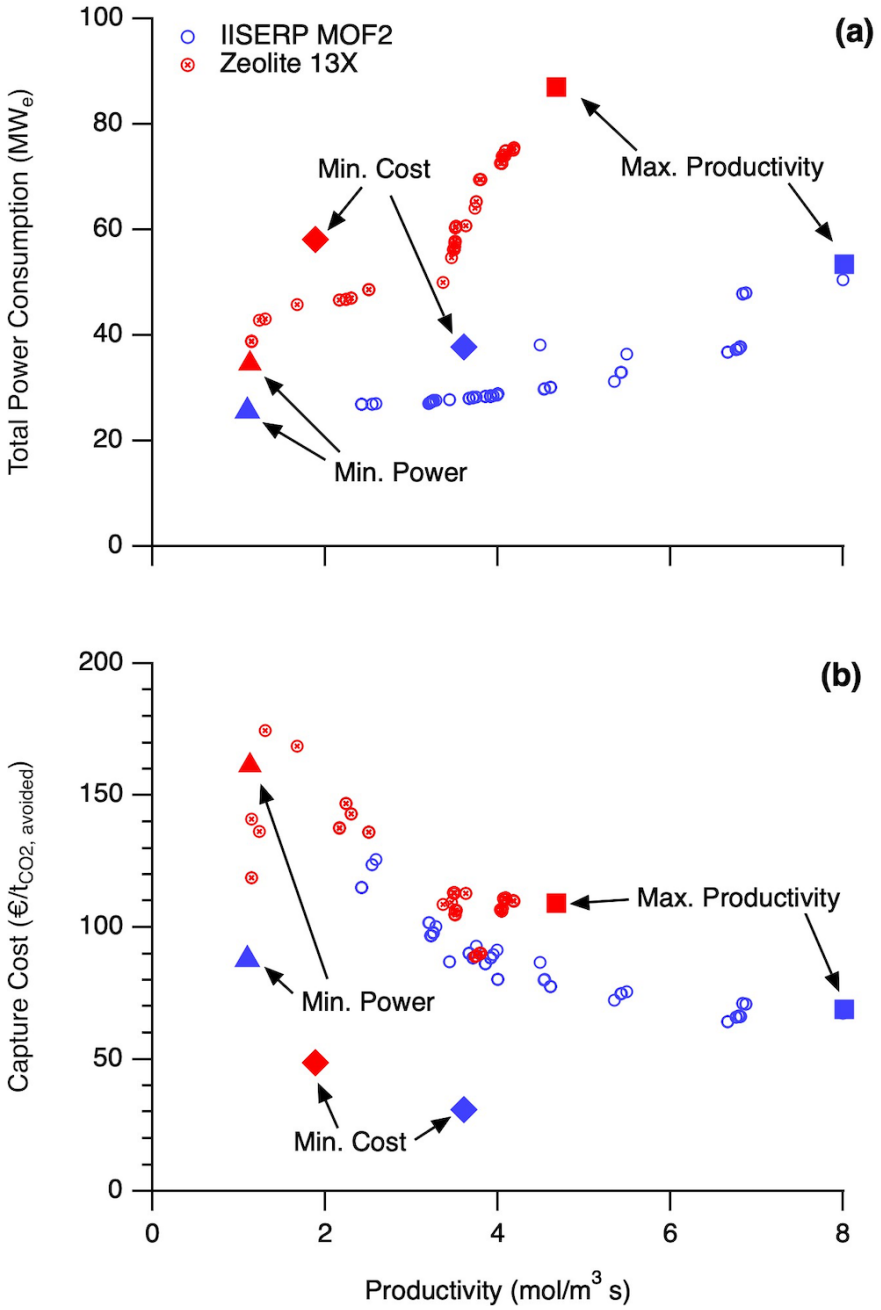

Figure 7: (a) Pareto solutions obtained from the multi-objective optimisation and (b) the corresponding capture costs for IISERP MOF2 (blue circles) and Zeolite 13X (red circles). For comparison, optimisation results pertaining to minimum capture cost (diamonds), minimum overall power consumption (triangles), maximum productivity (squares) are also illustrated.

This is the accepted version of an article published in Separation and Purification Technology
http://dx.doi.org/10.1016/j.seppur.2020.117832

4.3. Effect of overestimating the vacuum pump efficiency

Clearly, the costs linked to the electricity consumption influence the minimum overall capture cost. As the vacuum pump is a major power consumer, quantifying the realistic vacuum pump performance in terms of efficiency (η_V) is crucial. Most literature studies assume a constant theoretical $\eta_V \approx 70-80\%$ for VSA energy calculations, which, in practice, holds true for low to moderate vacuum levels ($\geq$0.1 bar). However, the production of high purity CO_2, at high recovery, based on VSA processes require deep vacuum pressures. To achieve deep vacuum (<0.1 bar), it was found in an earlier study that the vacuum pump performance significantly drops to a lower value [19]. This is also consistent with observations from pilot plant experiments [18]. The dependence of η_V on vacuum was regressed to formulate an efficiency function [19]. The same efficiency function was used in the present work, although not rigorous, captures the essential features of most of the vacuum pumps at deep vacuum. To understand the impact of η_V on the VSA process design and minimum capture cost, two optimisation cases are compared. The two cases considered are a fixed efficiency case where η_V=72% and a variable efficiency case η_V is a function of the pressure. The reference cases reported in Table 6 for IISERP MOF2 and Zeolite 13X are representative of variable η_V case. Independent optimisation runs were performed for both IISERP MOF2 and Zeolite 13X with η_V=72%.

The minimum capture cost results pertaining to constant η_V=72% case for both IISERP MOF2 and Zeolite 13X are presented as Case III in Table 8. For IISERP MOF2, the overall power consumption was estimated as 29.02 MW_e compared to 37.79 MW_e for the reference variable efficiency case. As expected, this difference primarily stems from the evacuation

step and translates to roughly 24% lower electricity costs. On the other hand, the overall power consumption for Zeolite 13X in the case of η_V=72% was underestimated by ≈20 MW_e (≈35%) as compared to that of the variable efficiency case. The productivity remained fairly constant as compared to reference cases for both materials. When the variable efficiency is considered for the vacuum pumps, the electricity consumption for IISERP MOF2 remained almost the same as that of the MEA-based capture case (see Table S1 in the Supporting Information) while Zeolite 13X demanded almost 1.5× the electricity needed for MEA case. On the contrary, the electricity consumption based on constant η_V=72% for IISERP MOF2 and Zeolite 13X remains ≈25% and ≈3%, respectively, lower than that of the MEA-based capture. This result corroborates the fact that the energy calculations based on theoretical vacuum pump efficiencies can optimistically lead to lower energy demands than that of MEA-based capture and moreover, can underestimate the realistic energy consumption [5].

As can be seen from Table 8, the vacuum pump efficiency directly influences the minimum capture cost. Using η_V=72% reduced the overall minimum capture cost by almost 8% and 17% for IISERP MOF2 and Zeolite 13X, respectively. As expected these savings come mainly from the reduction in OPEX related to electricity cost. While most other costs remained the same for IISERP MOF2, for Zeolite 13X the improved efficiency leads to a change in the VSA process design. It is interesting to notice that in the case of Zeolite 13X, some of the energy savings with η_V=72% goes towards increasing the column length leading to an increase in pressure drop. This leads reduction in number of parallel trains and the overall capital cost. Therefore, this study highlights the fact that an appropriate quantification of vacuum pump performance is important for calculating the realistic power

This is the accepted version of an article published in Separation and Purification Technology
http://dx.doi.org/10.1016/j.seppur.2020.117832

consumption, and thereby costs, of VSA processes.

This is the accepted version of an article published in Separation and Purification Technology
http://dx.doi.org/10.1016/j.seppur.2020.117832

Table 8: Techno-economic performances for case studies relating to the impact of the vacuum pump efficiency (Case III) and the length-to-diameter ratio (Case IV). Note that * indicates the change made with respect to reference cases in Tables 5 and 6.

	Case III	**Case III**	**Case IV**	**Case IV**
Adsorbent	Zeolite 13X	IISERP MOF2	Zeolite 13X	IISERP MOF2
Vacuum pump efficiency	72%*	72%*	Variable	Variable
Objective function	Min. Cost	Min. Cost	Min. Cost	Min. Cost
Operating Conditions				
Adsorption time (s)	235	117	189	119
Blowdown pump flow rate ($m^3\ h^{-1}$)	11922	4797	13549	17748
Evacuation pump flow rate ($m^3\ h^{-1}$)	19291	16638	14641	18482
Maximum feed pressure (bar)	2.14	2.00	1.69	1.97
Intermediate pressure (bar)	0.10	0.30	0.10	0.28
Low pressure (bar)	0.023	0.034	0.026	0.045
Feed velocity ($m\ s^{-1}$)	1.15	1.19	1.13	1.19
Column Length (m)	8.9	8.7	6.8	8.5
Length-to-diameter ratio (-)	3.0	3.0	2.0*	2.0*
Train Configuration				
Number of columns per train (-)	7	4	7	5
Blowdown pumps per train (-)	1	1	1	1
Evacuation pumps per train (-)	5	3	5	4
Number of parallel trains (-)	31	30	28	14
Process Performance				
Purity (%)	94.9	95.1	95.0	95.2
Recovery (%)	90.5	91.6	89.9	90.2
Productivity ($mol\ m^{-3}\ s^{-1}$)	1.82	3.58	2.03	2.87
Compressor power (MW_e)	13.90	13.53	9.69	13.37
Blowdown power (MW_e)	4.47	1.13	5.36	2.35
Evacuation power (MW_e)	19.29	14.36	31.86	16.57
Overall power consumption (MW_e)	37.66	29.02	46.91	32.29
Specific energy consumption (kWh_e/t_{CO_2})	200.67	152.75	251.55	172.51
Cost Performance				
CAPEX (€/$t_{CO_2,\ avoided}$)	17.3	11.3	15.8	10.9
Total Direct Cost (€/$t_{CO_2,\ avoided}$)	10.6	7.0	9.7	6.7
Column Cost (€/$t_{CO_2,\ avoided}$)	3.2	1.7	3.2	1.6
Compressor Cost (€/$t_{CO_2,\ avoided}$)	1.5	1.5	1.5	1.5
Vacuum Pump Cost (€/$t_{CO_2,\ avoided}$)	3.6	2.0	2.9	1.4
Heat Exchanger Cost (€/$t_{CO_2,\ avoided}$)	0.0	0.0	0.0	0.0
Valves Cost (€/$t_{CO_2,\ avoided}$)	0.3	0.1	0.3	0.1
Initial Adsorbent Cost (€/$t_{CO_2,\ avoided}$)	2.0	1.7	1.8	2.1
Process Contingency (€/$t_{CO_2,\ avoided}$)	1.6	1.0	1.5	1.0
Indirect Cost (€/$t_{CO_2,\ avoided}$)	1.7	1.1	1.6	1.1
Project Contingency (€/$t_{CO_2,\ avoided}$)	2.4	1.6	2.2	1.6
Owner Cost (€/$t_{CO_2,\ avoided}$)	0.9	0.6	0.8	0.5
OPEX (€/$t_{CO_2,\ avoided}$)	23.1	17.0	25.0	18.6
Fixed OPEX (€/$t_{CO_2,\ avoided}$)	8.4	5.6	7.7	5.4
Electricity Cost (€/$t_{CO_2,\ avoided}$)	11.7	8.9	14.7	10.1
Adsorbent Cost (€/$t_{CO_2,\ avoided}$)	2.8	2.3	2.5	2.9
Cooling Water Cost (€/$t_{CO_2,\ avoided}$)	0.2	0.2	0.1	0.2
VSA Capture Cost (€/$t_{CO_2,\ avoided}$)	**40.4**	**28.3**	**40.8**	**29.5**

This is the accepted version of an article published in Separation and Purification Technology
http://dx.doi.org/10.1016/j.seppur.2020.117832

4.4. Impact of length-to-diameter ratio

In this section, the effect of L/D ratio of adsorption columns on minimum capture cost was investigated by considering IISERP MOF2 and Zeolite 13X as case studies. While higher L/D ($\in \{4, 5\}$) could be considered for the analysis, previous simulations from the literature revealed that the high L/D may not favour the overall cost reduction [14]. Given the goal to reduce the overall CAPEX, lower $L/D \in \{2, 3\}$ were examined based on rigorous optimisations. The results shown in Table 6 for IISERP MOF2 and Zeolite 13X were considered as reference for L/D=3. The minimum capture costs corresponding to L/D=2, obtained after unique optimisation runs, are reported as Case IV in Table 8. As can be seen from the table, the size requirements of vacuum pumps have increased due to large diameters. Reducing the L/D ratio has demonstrated to have a limited effect on the minimum capture cost when using IISERP MOF2. The total number of columns reduced from 116 to 70 while the column costs remained constant. It is interesting to notice that the vacuum pump costs have reduced by ≈26% owing to fewer number of vacuum pumps. Contrarily, increase in adsorbent volume has resulted in increase in adsorbent costs by 28%. Therefore, the CAPEX remained nearly constant. Note that the electricity costs decreased by 14% because of the reduction in the power consumption mainly from the evacuation step (since P_{L} increased to 0.045 bar from 0.034 bar in the reference L/D=3 case). Overall, changing L/D from 3 to 2 has reduced the minimum capture cost from 30.8 to 29.5 € per tonne of CO_2 avoided.

The minimum capture cost was reduced to 40.8 € per tonne (lowered by ≈16%) for Zeolite 13X when the L/D was modified from 3 to 2. Clearly, there are a number of factors

contributing to the decrease in minimum capture cost. By using wider columns, the number of parallel trains reduced from 42 to 28 which also reduced the total number of columns from 294 to 196. This resulted in ≈16% reduction in column costs. Consequently, the adsorbent and valves costs have also decreased. Another contribution comes from fewer number of vacuum pumps. The vacuum pump costs have been lowered by ≈1.3× owing to 33% reduction in the total number of vacuum pumps. As a result, the CAPEX requirements were lowered by ≈15%. It is interesting to note that the overall power consumption reduced by ≈19% and also a 17% reduction in OPEX. Most industrial VSA columns in operation have reasonably large diameters indicating that wider columns can indeed be used to reduce the number of parallel trains and thereby cost of capture. Naturally, there should be a caution in terms of challenges related to implementation when designing wider columns such as those pertaining to flow distribution.

4.5. Comparative analysis with MEA-capture

Although MEA- and adsorption-based CO_2 capture technologies are on different levels of technological readiness levels, the key economic performance indicators were determined for both based on the assumption that the technologies are mature and ready for large-scale deployment. The cost performances of both technologies for post-combustion CCS implementation in SMR plants are illustrated in Fig. 8. The IISERP MOF2 cost performance reported in Table 6 was used as a representative case for VSA system in order to compare with reference MEA case. In addition, Zeolite 13X was also considered for the discussion as it represents the case for commercial adsorbents. Figure 8 shows the breakdown of CO_2

This is the accepted version of an article published in Separation and Purification Technology
http://dx.doi.org/10.1016/j.seppur.2020.117832

avoided costs (€/$t_{CO2,\ avoided}$) for CCS implementation of both technologies. As can be seen from the figure, CO_2 avoided cost for VSA based on IISERP MOF2 is almost 10% higher than that of the MEA case. The VSA performance with Zeolite 13X deteriorates further with a CO_2 avoided cost of 90.9 € per tonne of CO_2 avoided. It is worth noting that the CO_2 capture remains the major contributor for CCS implementation in both technologies. For MEA-based absorption, the CO_2 capture costs were determined to be 30.1 € per tonne of CO_2 avoided [21]. The capture costs for VSA system based on IISERP MOF2 are 12% higher than that of MEA-based capture whereas 71% higher when Zeolite 13X is used. Note that the capture costs for VSA also include flue gas cooling and drying costs. The CO_2 conditioning, transport and storage costs are marginally higher (i.e. <10%) for VSA because of slightly higher flow rates as compared to that of the MEA case. Upon close examination of capture costs, the components responsible for higher capture costs for VSA system include CAPEX, fixed OPEX and costs linked to energy consumption, as illustrated in Fig. 8. The VSA-based capture based on IISERP MOF2 and Zeolite 13X results in 7% and 68% higher CAPEX, respectively, as compared to the MEA case, due to the large number of parallel trains and associated footprint together with flue gas pre-treatment. This shows that MOFs have ability to significantly reduce the huge capital costs. The fixed operating costs, which depend on the total capital requirement, are 21% higher in VSA system that is based on IISERP MOF2 when compared to reference MEA case. Finally, the costs linked to electricity consumption for capture are again 15% and 77% higher in the VSA cases for IISERP MOF2 and Zeolite 13X, respectively, which comes from the power consumption due to requirement of low vacuum levels and a large number of vacuum pumps. This is an interesting result be-

cause VSA-based processes are often reported as low energy intensive processes for capture. While most of the studies assume high vacuum pump efficiencies at deep vacuum, the practical limitations of vacuum pumps at deep vacuum are often overlooked. The analysis related to fixing the vacuum pump efficiency in the earlier section showed that the energy numbers for the VSA process are indeed lower than that of the MEA-based capture. Altogether, the MEA-based capture outperforms four-step VSA process based on the adsorbents considered in terms of the CO_2 avoided cost for post-combustion CO_2 capture in SMR plants.

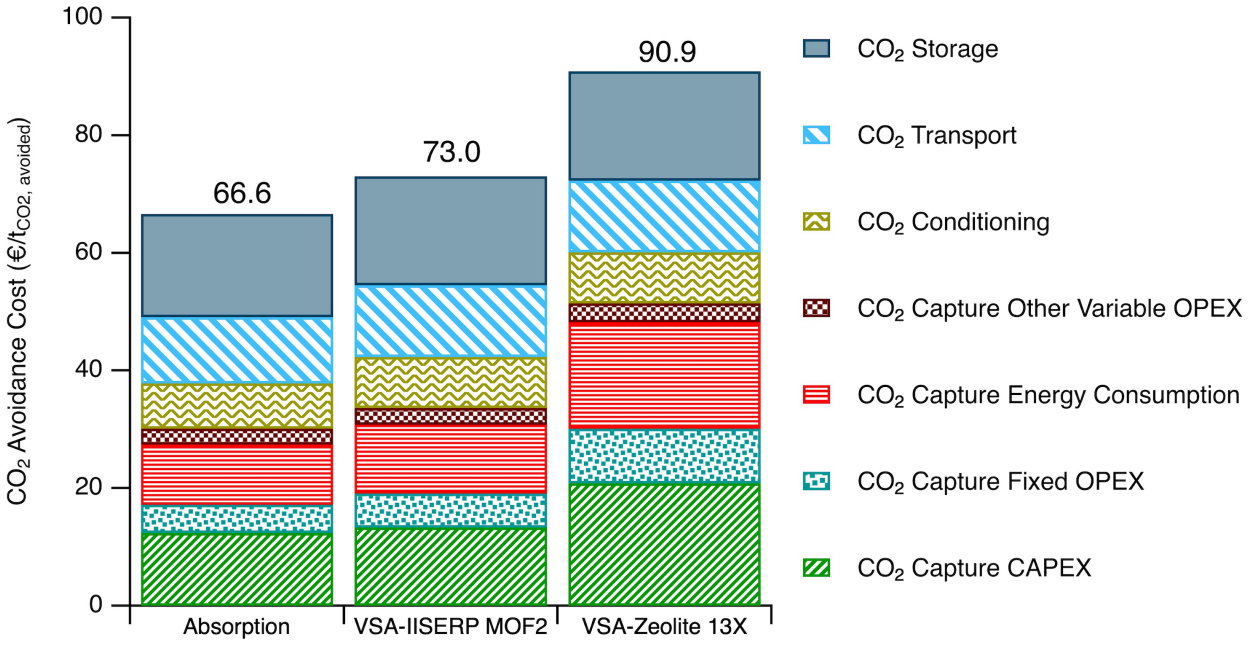

Figure 8: Cost performance of the VSA technology as compared to MEA solvent for CCS implementation. Note that VSA-based CO_2 capture also includes cooling and drying costs.

4.6. Cost of Metal-Organic Frameworks

As mentioned earlier, given the wide uncertainties involved in the large-scale production of metal-organic frameworks, estimating an actual price remains a critical challenge while

This is the accepted version of an article published in Separation and Purification Technology
http://dx.doi.org/10.1016/j.seppur.2020.117832

evaluating the techno-economic feasibility of MOFs for CO_2 capture. Although cost estimations based on the raw materials provide a reasonable approximation for purchase costs, the scale-up for CCS application is expected to reduce the production costs for MOFs. Given such variability of MOF prices, it is important to understand the MOF price for which adsorption processes are attractive. To this end, the influence of MOF price on the CO_2 capture cost was examined through an optimisation study where the VSA process was optimised for the minimum capture cost for different MOF prices. Both UTSA-16 and IISERP MOF2 were considered for the analysis as each MOF represents a unique scenario. The synthesis of UTSA-16 involves an expensive metal source, cobalt, as the raw material while IISERP MOF2 composes of comparatively cheaper metal, nickel. The MOF price was varied over a broad range of 0 and 10 times the cost of relative metal content. In each case, unique optimisation runs were performed for both IISERP MOF2 and UTSA-16 and minimum capture costs were determined. The minimum cost performances of UTSA-16 and IISERP MOF2 presented in Table 6 represent a baseline case where the MOF price assumed was twice the cost of the relative metal content in the MOF structure.

Figure 9 shows the overall trend of MOF price on the minimum cost of capture. Every point on the figure represents a unique optimisation run. Note that optimisation runs corresponding to zero MOF price are shown at the left most portion of the plot. A MOF price of zero indicates that the MOF is available for use at no cost. Although, never encountered in practice, it provides the absolute lower bound for this case study. A factor of $1\times$ represents a case where the production cost equals the cost of bulk purchase of metals and the cost of organic linkers, solvents and other production costs are negligible subject to the economics

This is the accepted version of an article published in Separation and Purification Technology
http://dx.doi.org/10.1016/j.seppur.2020.117832

of scale. In other words, 1× is the lowest possible estimate that can be practically achieved when the MOF price is same as the raw materials cost. On the other hand, a worst case situation involves MOF price amounting to 10 times the metal purchase cost which is a representative case of poor scale-up. For UTSA-16, the minimum capture cost increases as the MOF price increases. As can be seen from Fig. 9, the UTSA-16 prices vary between 0 € and 83200 € per tonne. Clearly, higher UTSA-16 costs discourage the practical implementation in a VSA process. Such exorbitant costs can be attributed to the presence of expensive metal source, cobalt. The advantages UTSA-16 offers in terms of process performance are limited by its expected price. As can be seen from Fig. 9, a slight reduction in the MOF price leads to a significant decrease in the overall capture cost. It is worth noting that the UTSA-16 performs better than commercial adsorbent like Zeolite 13X when the production costs are as close as zero, but still is expensive compared to MEA-capture. For this case of zero price, it is worth mentioning that both the column length and the interstitial feed velocity have approached the upper limit as the optimiser was seeking to reduce the number of parallel trains, which otherwise was impeded by exorbitant adsorbent costs. IISERP MOF2 prices, on the other hand, were varied between 0 € and € 22200 per tonne. As expected, higher IISERP MOF2 price resulted in gradual increase in minimum capture cost. As can be seen from Fig. 9, IISERP MOF2 always outperforms Zeolite 13X over this broad range. It is also interesting to notice that the IISERP MOF2 outperforms reference MEA-capture case when the price IISERP MOF2 price is less than 1×, i.e less than the raw materials cost. However, caution should be used in this regard as the MEA is the baseline case, although other solvents can lead to lower capture costs. The overall trend suggests that the MOF's

superior technical performance outperforms the cost characteristics when the metal sources are cheap and available in abundance. The deployment of MOFs, especially with expensive metals, seems to be prohibitive. It is therefore important to search for high performance adsorbents that are cheaply available.

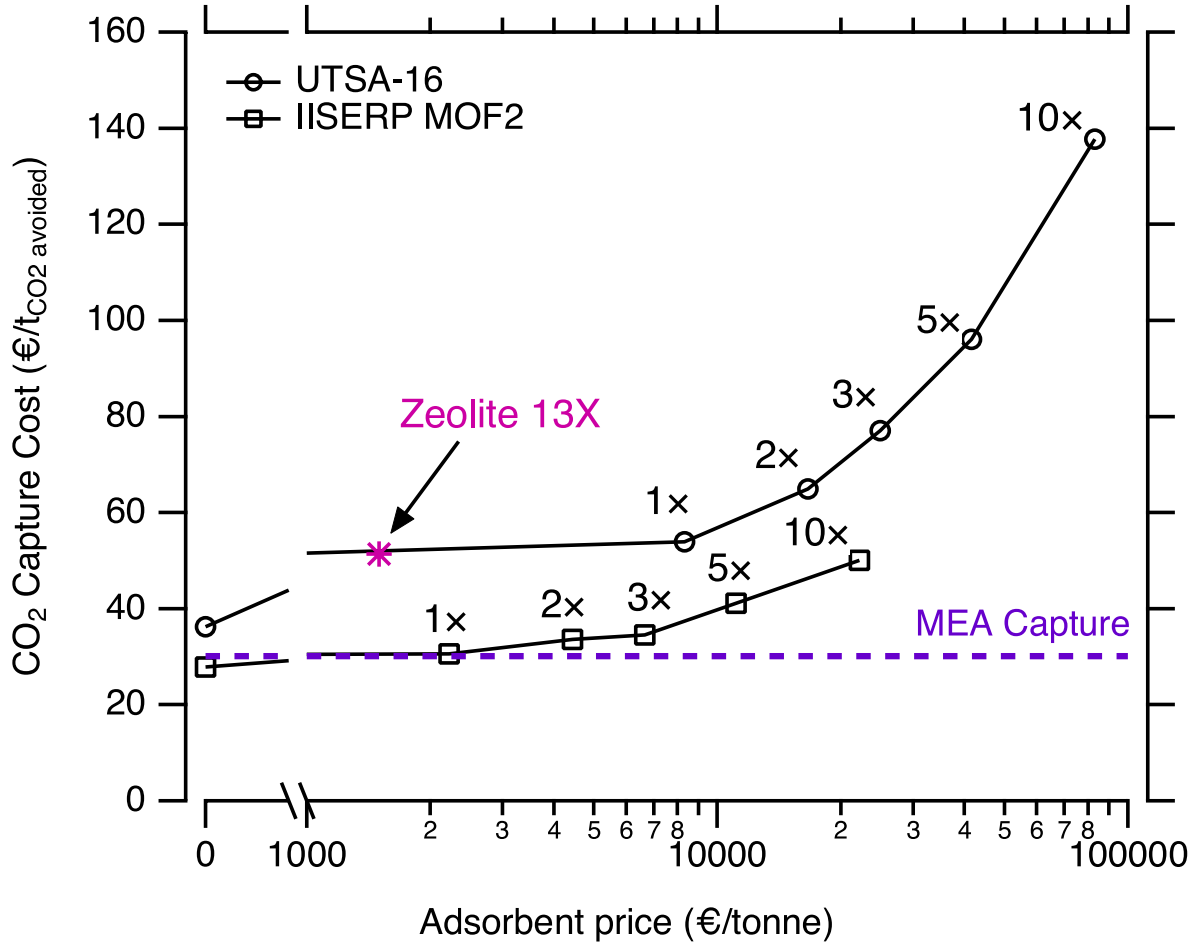

Figure 9: Influence of adsorbent prices on the minimum CO_2 capture cost (includes cooling and drying costs for VSA). Zeolite 13X and MEA-capture costs are shown for reference. The indicators, 1×, 2×, ..., 10×, refer to the multiplier applied to the cost of the metal in the metal-organic framework.

This is the accepted version of an article published in Separation and Purification Technology
http://dx.doi.org/10.1016/j.seppur.2020.117832

5. Conclusions and Perspectives

A systematic approach for the design and techno-economic assessment of vacuum swing adsorption (VSA) processes was developed. The methodology incorporates detailed VSA process model, peripheral component models, vacuum pump performance, scale-up, process scheduling and comprehensive costing model including cost of adsorbent. This methodology was applied to a case study on post-combustion CO_2 capture from a Steam Methane Reformer (SMR).

An integrated techno-economic methodology, consistent with best practices, combined with stochastic optimization, was used to calculate the minimum CO_2 capture cost and the corresponding process design and operating parameters. The key results of the work can be summarized as follows:

- Optimizing the VSA process for proxy objectives such as minimizing energy and maximizing productivity does not guarantee the minimum cost. The minimum cost configurations did not lie on the minimum-energy vs maximum-productivity Pareto curves. This arises because of the complexities that exist in the scale-up of VSA processes from single-column simulations, a technique commonly used in the literature.

- The study clearly shows that the realistic efficiencies for vacuum pumps, especially at low pressures, need to be accounted for in order to obtain better estimates of the capture cost. It was shown that efficiencies that are used in literature, typically $\approx 72\%$, can indeed underestimate the overall power consumption as much as 24- 35% resulting in 8 - 17% lower minimum capture cost for specific cases in this work.

This is the accepted version of an article published in Separation and Purification Technology
http://dx.doi.org/10.1016/j.seppur.2020.117832

- The choice of adsorbent and its cost has a major impact on the cost of CO_2 capture. Three different adsorbents that include, Zeolite 13X and metal-organic frameworks, UTSA-16 and IISERP MOF2, were compared based on minimum CO_2 capture costs and benchmarked against state-of-the-art MEA-based absorption process. IISERP MOF2 was found out to be the best performing adsorbent with a minimum CO_2 capture cost of 33.6 € per tonne of CO_2 avoided, inclusive of flue gas pre-treatment costs. The current benchmark adsorbent material, Zeolite 13X, ranked second with a minimum capture cost of 51.4 € per tonne of CO_2 avoided. A higher power consumption and a lower productivity resulted in higher overall costs for Zeolite 13X. UTSA-16 remains performing poorly with a minimum capture cost 64.9 € per tonne of CO_2 avoided, primarily, due to exorbitant adsorbent costs. The presence of expensive metal source, cobalt, inhibited the superior technical performance of UTSA-16.

- Adsorbents that were found to be better candidates based on their superior energy/productivity performance did not necessarily result in lower cost. For instance, UTSA-16, which has consistently been touted as an excellent candidate for CO_2 capture compared to the benchmark material Zeolite 13X, did not provide better cost performance. This was clearly shown to be a direct result of exorbitant adsorbent cost.

- The baseline MEA outperforms the best performing adsorbent IISERP MOF2 with 10% lower CO_2 avoided cost. The MOF prices were varied over a wide range, given the variability in MOF scale-up, to comprehend the potential production costs at

This is the accepted version of an article published in Separation and Purification Technology
http://dx.doi.org/10.1016/j.seppur.2020.117832

which MOF gives advantage over commercial adsorbent like Zeolite 13X and the baseline MEA process. It was shown that UTSA-16 outperforms Zeolite 13X only when its production costs are less than the costs of raw materials, a seemingly impossible proposition. On the other hand, capture costs for IISERP MOF2 are less than Zeolite 13X over the entire range considered and on par with reference MEA-capture when IISERP MOF2 prices are almost equal to the raw material costs.

The study provides some key perspectives when considering vacuum swing adsorption processes for CO_2 capture:

- When the system is to be operated in the vacuum swing adsorption mode, deep vacuum pressures, i.e., < 0.1 bar seem unavoidable. This seems to arise from the high purity and recovery constraints that are enforced on the separation.

- In the VSA mode, using beaded adsorbents, it is challenging to compete with MEA processes. The key limitation comes from the maximum velocities that are employable in these systems. This results in the requirement of a large number of columns and multiple parallel trains. While a certain level of robustness can be anticipated from the use of multiple modules, they present two major challenges. The first one is that of complexity. Integrating the number of modules and dealing with the associate piping and control systems can be challenging. The second one is that of the cost. Since multiplexing seems to be unavoidable, it is difficult to anticipate savings from "economies of scale". Therefore, this also emphasizes that the scale of the capture plant is an important factor to be considered. Owing to the reduced level of complexity

and cost competitiveness with other technologies, the VSA technology may remain attractive at small and mid-scale point sources.

- Naturally, the study should be viewed in terms of the design philosophy and physical constraints, e.g., L/D ratios, maximum velocities, vacuum pump efficiencies, before drawing sweeping conclusions. This means that future adsorption-based studies should focus on drastically different approaches, for instance, the use of monoliths or parallel-passage contacts coupled with rapid cycling, the use of better adsorbents that can be manufactured in large-quantities using earth-abundant materials, other cycles, etc.

Supporting Information

Details of hydrogen plant with post-combustion MEA-based CO_2 capture; set of governing equations and boundary conditions related to VSA; VSA simulation parameters; dual-site Langmuir isotherm parameters for the three adsorbents; details for calculating number of columns per train, vacuum pumps per train and number of parallel trains; technical modelling of compressors, vacuum pumps and heat exchangers; details of flue gas cooling and drying, CO_2 conditioning, transport and storage and; optimal column scheduling for the three adsorbents.

Acknowledgements

This publication has been produced with support from the NCCS Centre, performed under the Norwegian research program Centres for Environment-friendly Energy Research

(FME). The authors acknowledge the following partners for their contributions: Aker Solutions, Ansaldo Energia, Baker Hughes, CoorsTek Membrane Sciences, EMGS, Equinor, Gassco, Krohne, Larvik Shipping, Lundin, Norcem, Norwegian Oil and Gas, Quad Geometrics, Total, Vår Energi, and the Research Council of Norway (257579/E20). Funding from Canada First Research Excellence Fund through University of Alberta Future Energy Systems is acknowledged. All computations reported in this work were supported by Compute Canada's Resources for Research group grant.

Appendix A. Appendix: Direct cost functions for process equipment

The direct costs of individual process equipment were estimated using Aspen Economic Process Analyzer®. Several economic evaluations were performed for each equipment based on a wide range of key design characteristics in order to develop reliable direct cost functions for the optimisation. DataFit was used to carry out the regression and it was ensured that the obtained direct cost functions are continuous in the ranges used for the optimisation. It is worth mentioning that a design margin of 1.1 in the flows was used at the desired pressure and temperature for the evaluations. However, the regressions are always related to operating conditions without design margins. More details on the regression including the adjusted coefficient of multiple determination (R^2_{ADJ}), average absolute error (avg. abs. error) and maximum absolute error (max. abs. error) are summarized below.

A.1. Columns

In an attempt to develop a generic direct cost function for columns, 156 cases with a wide range of characteristics were considered. Economic evaluations were performed for different

diameters, length-to-diameter (L/D) ratios and pressures. The direct cost function based on three variables is given in Eq. A.1. The obtained regression parameters are provided in Table A1. Figure A1 illustrates the regression.

$$\text{Column direct cost } (€) = \exp(a \cdot \text{Diameter (m)} + b \cdot L/D \text{ (-)} + c \cdot \text{Pressure (bar)} + d) \quad \text{(A.1)}$$

Table A1: Regression characteristics of columns

Parameter	**Column**
Coefficient a	0.4148138
Coefficient b	0.0738133
Coefficient c	0.0231138
Coefficient d	10.807870
R^2_{ADJ}	0.986
Avg. abs. error (%)	4.71
Max. abs. error (%)	15.74
Number of cases evaluated	156
Diameter range (m)	1-5
Length-to-Diameter Ratio range (-)	2-6
Pressure range (bar)	1-4

This is the accepted version of an article published in Separation and Purification Technology
http://dx.doi.org/10.1016/j.seppur.2020.117832

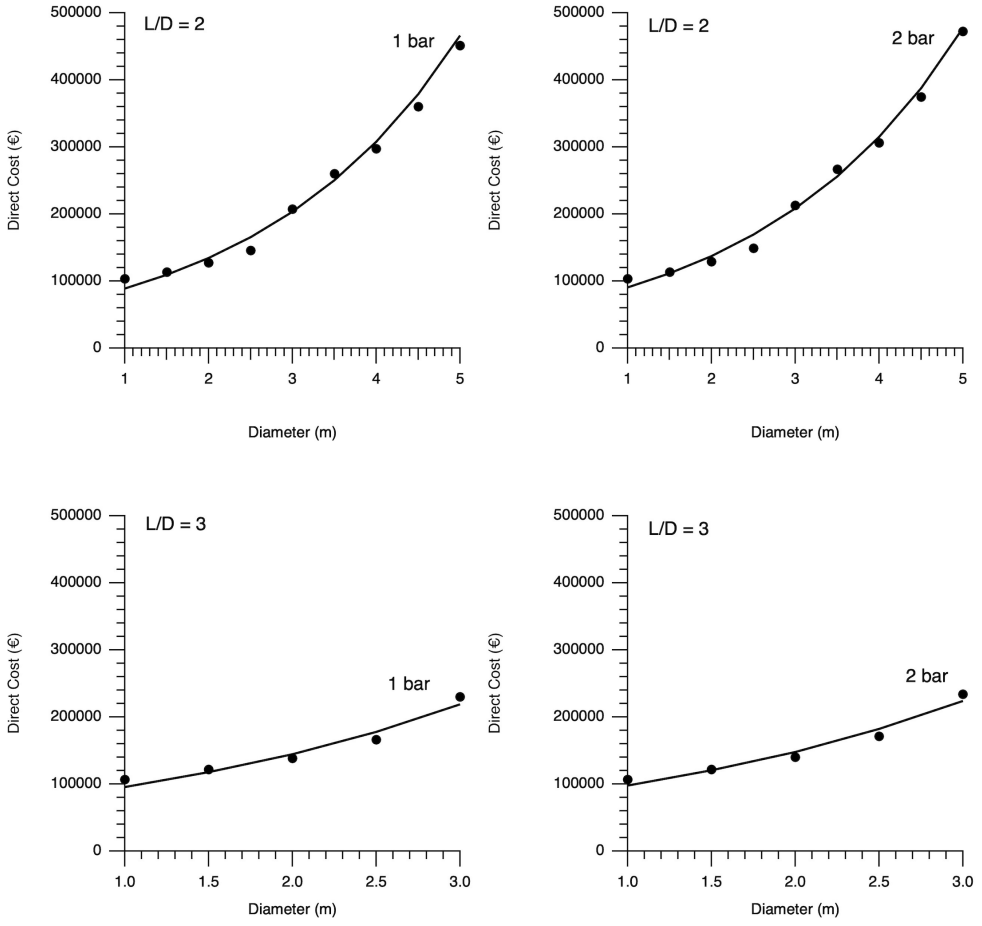

(a)

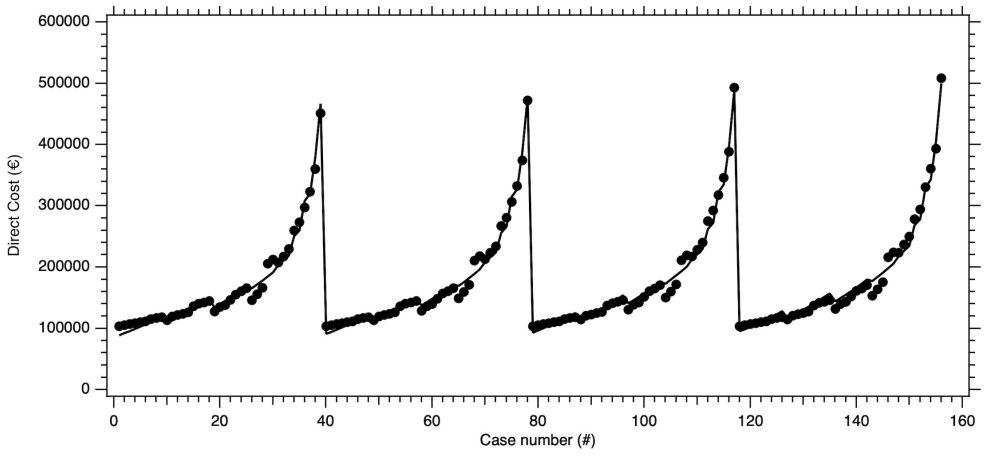

(b)

Figure A1: Direct cost regression of columns. Note that the points represent the Aspen Economic Process Analyzer® evaluations and the lines are regressed cost functions.

This is the accepted version of an article published in Separation and Purification Technology
http://dx.doi.org/10.1016/j.seppur.2020.117832

A.2. Compressors

Based on 63 evaluations, a two-variable direct cost function was obtained for single-stage compressors as shown in Eq. A.2. Actual inlet volumetric flow rate and outlet pressure were varied to represent accurate cost estimations for compressors. The obtained regression parameters and characteristics are listed in Table A2, while Fig. A2 shows the regression.

$$\text{Compressor direct cost } (€) = a \cdot \left(\text{Inlet flow rate } (\text{m}^3\ \text{h}^{-1}\ )\right)^b \cdot c^{\text{Pressure (bar)}} \tag{A.2}$$

Table A2: Regression characteristics of rotating equipment

Parameter	**Compressor**	**Vacuum Pump**
Coefficient a	121.412	423.900
Coefficient b	0.900	0.653
Coefficient c	1.032	30000.000
R^2_{ADJ}	0.998	0.999
Avg. abs. error (%)	1.43	0.61
Max. abs. error (%)	3.95	1.94
Number of cases evaluated	63	19
Flow range ($\text{m}^3\ \text{h}^{-1}$)	100000-500000	250-20000
Pressure range (bar)	1-4	0.01-1

This is the accepted version of an article published in Separation and Purification Technology
http://dx.doi.org/10.1016/j.seppur.2020.117832

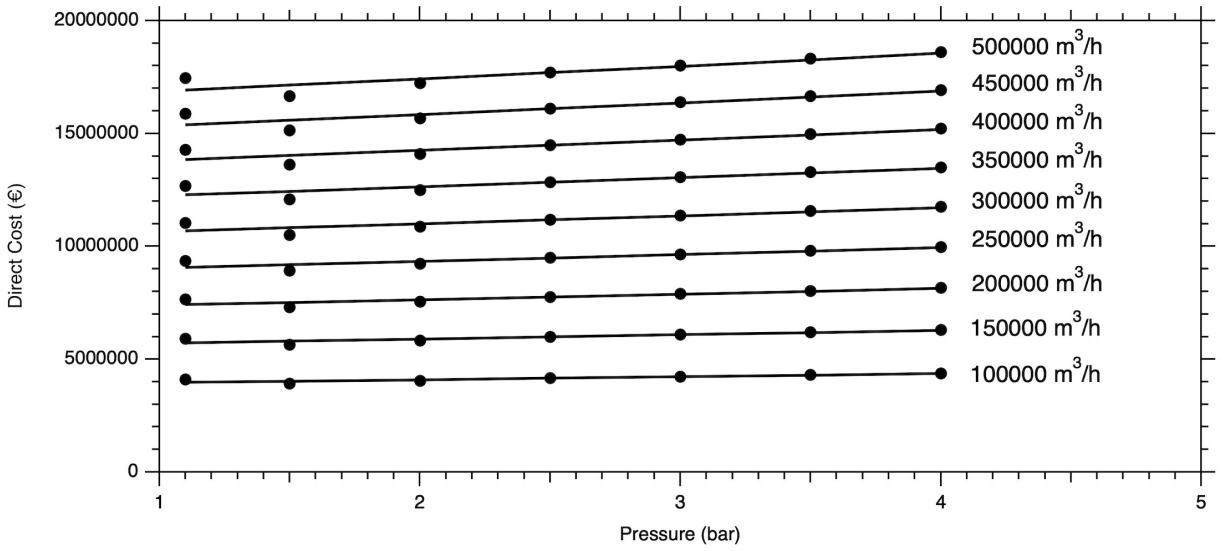

(a)

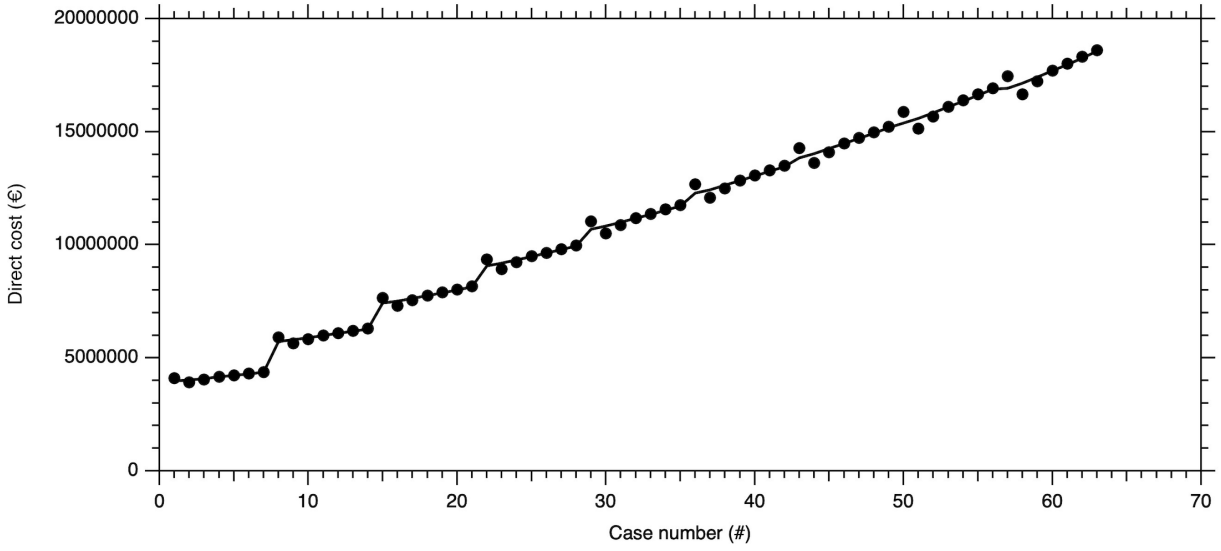

(b)

Figure A2: Direct cost regression of compressors. Note that the points represent the Aspen Economic Process Analyzer® evaluations and the lines are regressed cost functions.

A.3. Vacuum Pump

For a reliable vacuum pump direct cost estimation, 19 cases were considered for economic evaluation in Aspen Economic Process Analyzer®. The key design characteristics of the

This is the accepted version of an article published in Separation and Purification Technology
http://dx.doi.org/10.1016/j.seppur.2020.117832

vacuum pump include the volumetric flow rate and the suction pressure. The cases are representative of a wide span of volumetric flow rates. For all the cases, the suction pressure operating range remains the same, between 0.01 bar and 1 bar. Hence, a direct cost function with volumetric flow rate was regressed as shown in Eq. A.3. The regression parameters and characteristics can be found in Table A2, while the regression is shown in Fig. A3.

$$\text{Vacuum Pump direct cost } (€) = a \cdot \left(\text{Inlet flow rate } (\text{m}^3\ \text{h}^{-1})\right)^b + c \tag{A.3}$$

This is the accepted version of an article published in Separation and Purification Technology
http://dx.doi.org/10.1016/j.seppur.2020.117832

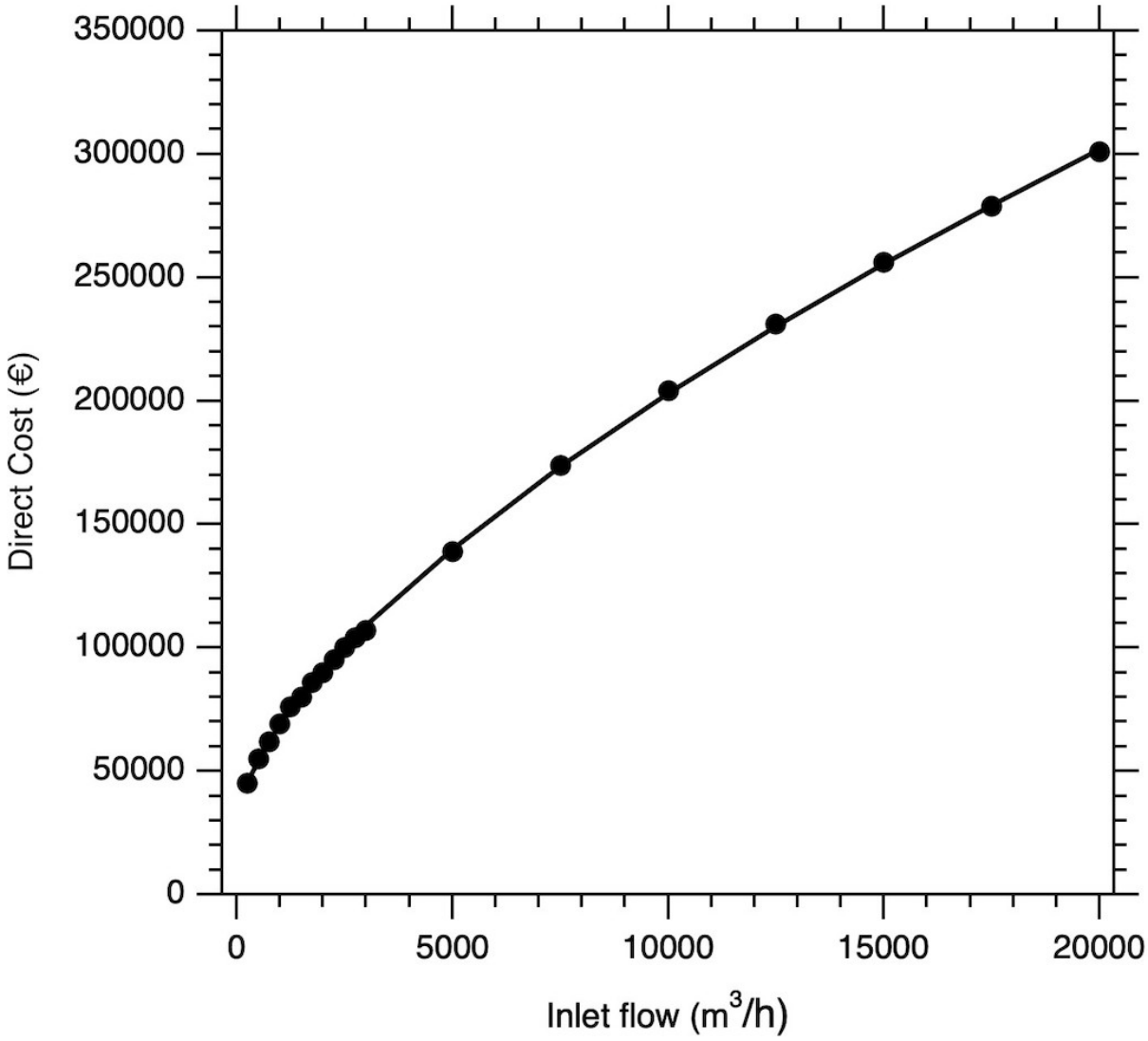

Figure A3: Direct cost regression of vacuum pumps. Note that the points represent the Aspen Economic Process Analyzer® evaluations and the lines are regressed cost functions.

A.4. Heat Exchangers

The direct cost function of heat exchangers with both heat exchange area and pressure as variables was obtained from Deng et. al [43]. Suitable factors were used to update costs to €$_{2016}$ using Chemical Engineering Plant Cost Index (CEPCI) and inflation. The two-variable cost function is shown in Eq. A.4 and the regression parameters are provided in

This is the accepted version of an article published in Separation and Purification Technology
http://dx.doi.org/10.1016/j.seppur.2020.117832

Table A3.

$$\text{Heat exchanger direct cost } (€) = a \cdot \left(\text{Area } (\text{m}^2)\right)^b \cdot c^{\text{Pressure (bar)}} \tag{A.4}$$

Table A3: Regression characteristics of heat exchangers [43]

Parameter	**Heat Exchanger**
Coefficient a	12003
Coefficient b	0.603
Coefficient c	1.011187
R^2_{ADJ}	0.959
Avg. abs. error (%)	14.2
Max. abs. error (%)	32.6
Number of cases evaluated	53
Area range (m^2)	30-4000
Pressure range (bar)	2.7-81

A.5. Switching Valves

Owing to the cyclic nature of the VSA operation, switching valves are essential to implement the cycle sequence. Based on the VSA cycle considered, the number of switching valves required per column was estimated to be 3. Given the several number of columns required to capture the flue gas, the cost of valves will no longer be insignificant. Hence, the direct cost of each valve was set to 6000 €. Note that the valves related to the control and instrumentation are accounted for in the indirect costs of process equipment.

This is the accepted version of an article published in Separation and Purification Technology
http://dx.doi.org/10.1016/j.seppur.2020.117832

A.6. Adsorbent Costs

The adsorbent direct costs comprise purchase costs (PC) and transport and installation costs (TIC) and were calculated as follows:

$$\text{Adsorbent direct cost } (€) = M \cdot N \cdot \text{Column Volume} \cdot (1-\varepsilon) \cdot \rho_s \cdot (PC + TIC) \quad \text{(A.5)}$$

This is the accepted version of an article published in Separation and Purification Technology
http://dx.doi.org/10.1016/j.seppur.2020.117832

References

[1] Voldsund, M.; Jordal, K.; Anantharaman, R. Hydrogen production with CO_2 capture. *Int. J. Hydrogen Energy* **2016**, *41*, 4969 – 4992.

[2] IEA, Technology roadmap - Hydrogen and fuel cells. IEA, Paris, 2015.

[3] IEAGHG, Techno-economic evaluation of SMR based standalone (merchant) plant with CCS, 2017/02. February 2017.

[4] Meerman, J.; Hamborg, E.; van Keulen, T.; Ramírez, A.; Turkenburg, W.; Faaij, A. Techno-economic assessment of CO_2 capture at steam methane reforming facilities using commercially available technology. *Int. J. Greenh. Gas Control* **2012**, *9*, 160 – 171.

[5] Bui, M. et al. Carbon capture and storage (CCS): the way forward. *Energy Environ. Sci.* **2018**, *11*, 1062–1176.

[6] IEAGHG, The carbon capture project at Air Products' Port Arthur hydrogen production facility, 2018/05. December 2018.

[7] Rajagopalan, A. K.; Avila, A. M.; Rajendran, A. Do adsorbent screening metrics predict process performance? A process optimisation based study for post-combustion capture of CO_2. *Int. J Greenh. Gas Control* **2016**, *46*, 76 – 85.

[8] Nikolaidis, G. N.; Kikkinides, E. S.; Georgiadis, M. C. Model-based approach for the evaluation of materials and processes for post-combustion carbon dioxide capture from flue gas by PSA/VSA processes. *Ind. Eng. Chem. Res.* **2016**, *55*, 635–646.

[9] Leperi, K. T.; Chung, Y. G.; You, F.; Snurr, R. Q. Development of a general evaluation metric for rapid screening of adsorbent materials for postcombustion CO_2 capture. *ACS Sustain. Chem. Eng.* **2019**, *7*, 11529–11539.

[10] Yancy-Caballero, D.; Leperi, K. T.; Bucior, B. J.; Richardson, R. K.; Islamoglu, T.; Farha, O. K.; You, F.; Snurr, R. Q. Process-level modelling and optimization to evaluate metal–organic frameworks for post-combustion capture of CO_2. *Mol. Syst. Des. Eng.* **2020**, *5*, 1205–1218.

[11] Haghpanah, R.; Nilam, R.; Rajendran, A.; Farooq, S.; Karimi, I. A. Cycle synthesis and optimization

This is the accepted version of an article published in Separation and Purification Technology
http://dx.doi.org/10.1016/j.seppur.2020.117832

of a VSA process for postcombustion CO_2 capture. *AIChE J.* **2013**, *59*, 4735–4748.

[12] Ho, M. T.; Allinson, G. W.; Wiley, D. E. Reducing the cost of CO_2 capture from flue gases using pressure swing adsorption. *Ind. Eng. Chem. Res.* **2008**, *47*, 4883–4890.

[13] Hasan, M. M. F.; Baliban, R. C.; Elia, J. A.; Floudas, C. A. Modeling, simulation, and optimization of postcombustion CO_2 capture for variable feed concentration and flow rate. 2. Pressure swing adsorption and vacuum swing adsorption processes. *Ind. Eng. Chem. Res.* **2012**, *51*, 15665–15682.

[14] Susarla, N.; Haghpanah, R.; Karimi, I.; Farooq, S.; Rajendran, A.; Tan, L. S. C.; Lim, J. S. T. Energy and cost estimates for capturing CO_2 from a dry flue gas using pressure/vacuum swing adsorption. *Chem. Eng. Res. Des.* **2015**, *102*, 354 – 367.

[15] Leperi, K. T.; Snurr, R. Q.; You, F. Optimization of two-stage pressure/vacuum swing adsorption with variable dehydration level for postcombustion carbon capture. *Ind. Eng. Chem. Res.* **2016**, *55*, 3338–3350.

[16] Khurana, M.; Farooq, S. Integrated adsorbent process optimization for minimum cost of electricity including carbon Capture by a VSA process. *AIChE J.* **2019**, *65*, 184–195.

[17] Danaci, D.; Bui, M.; Mac Dowell, N.; Petit, C. Exploring the limits of adsorption-based CO_2 capture using MOFs with PVSA – from molecular design to process economics. *Mol. Syst. Des. Eng.* **2020**, *5*, 212–231.

[18] Krishnamurthy, S.; Rao, V. R.; Guntuka, S.; Sharratt, P.; Haghpanah, R.; Rajendran, A.; Amanullah, M.; Karimi, I. A.; Farooq, S. CO_2 capture from dry flue gas by vacuum swing adsorption: A pilot plant study. *AIChE J.* **2014**, *60*, 1830 –1842.

[19] Maruyama, R. T.; Pai, K. N.; Subraveti, S. G.; Rajendran, A. Improving the performance of vacuum swing adsorption based CO_2 capture under reduced recovery requirements. *Int. J. of Greenh. Gas Control* **2020**, *93*, 102902.

[20] Roussanaly, S.; Anantharaman, R.; Lindqvist, K.; Hagen, B. A new approach to the identification of high-potential materials for cost-efficient membrane-based post-combustion CO_2 capture. *Sustain. Energy Fuels* **2018**, *2*, 1225–1243.

This is the accepted version of an article published in Separation and Purification Technology
http://dx.doi.org/10.1016/j.seppur.2020.117832

[21] Roussanaly, S.; Anantharaman, R.; Fu., C. Low-carbon footprint hydrogen production from natural gas: A techno-economic analysis of carbon capture and storage from steam-methane reforming. *Chem. Eng. Trans.* **2020**, *81*, 1015–1020.

[22] Khurana, M.; Farooq, S. Integrated adsorbent-process optimization for carbon capture and concentration using vacuum swing adsorption cycles. *AIChE J* **2017**, *63*, 2987–2995.

[23] Farmahini, A. H.; Krishnamurthy, S.; Friedrich, D.; Brandani, S.; Sarkisov, L. From crystal to adsorption column: Challenges in multiscale computational screening of materials for adsorption separation processes. *Ind. Eng. Chem. Res.* **2018**, *57*, 15491–15511.

[24] Farmahini, A. H; Friedrich, D.; Brandani, S.; Sarkisov, L. Exploring new sources of efficiency in process-driven materials screening for post-combustion carbon capture. *Energy Environ. Sci.* **2020**, *13*, 1018–1037.

[25] Haghpanah, R.; Majumder, A.; Nilam, R.; Rajendran, A.; Farooq, S.; Karimi, I. A.; Amanullah, M. Multiobjective optimization of a four-step adsorption process for postcombustion CO_2 capture via finite volume simulation. *Ind. Eng. Chem. Res* **2013**, *52*, 4249–4265.

[26] Xiao, P.; Zhang, J.; Webley, P.; Li, G.; Singh, R.; Todd, R. Capture of CO_2 from flue gas streams with Zeolite 13X by vacuum-pressure swing adsorption. *Adsorption* **2008**, *14*, 575–582.

[27] Xiang, S.; He, Y.; Zhang, Z.; Wu, H.; Zhou, W.; Krishna, R.; Chen, B. Microporous metal-organic framework with potential for carbon dioxide capture at ambient conditions. *Nat. Commun.* **2012**, *3*, 954.

[28] Agueda, V. I.; Delgado, J. A.; Uguina, M. A.; Brea, P.; Spjelkavik, A. I.; Blom, R.; Grande, C. Adsorption and diffusion of H_2, N_2, CO, CH_4 and CO_2 in UTSA-16 metal-organic framework extrudates. *Chem. Eng. Sci.* **2015**, *124*, 159 – 169.

[29] Nandi, S.; Collins, S.; Chakraborty, D.; Banerjee, D.; Thallapally, P. K.; Woo, T. K.; Vaidhyanathan, R. Ultralow parasitic energy for postcombustion CO_2 capture realized in a nickel isonicotinate metal–organic framework with excellent moisture stability. *J. Am. Chem. Soc.* **2017**, *139*, 1734–1737.

This is the accepted version of an article published in Separation and Purification Technology
http://dx.doi.org/10.1016/j.seppur.2020.117832

[30] Burns, T. D.; Pai, K. N.; Subraveti, S. G.; Collins, S. P.; Krykunov, M.; Rajendran, A.; Woo, T. K. Prediction of MOF performance in vacuum swing adsorption systems for postcombustion CO_2 capture based on integrated molecular simulations, process optimizations, and machine learning models. *Environ. Sci. Technol.* **2020**, *54*, 4536–4544.

[31] Perez, L. E.; Sarkar, P.; Rajendran, A. Experimental validation of multi-objective optimization techniques for design of vacuum swing adsorption processes. *Sep. Purif. Technol.* **2019**, *224*, 553 – 563.

[32] Subraveti, S. G.; Pai, K. N.; Rajagopalan, A. K.; Wilkins, N. S.; Rajendran, A.; Jayaraman, A.; Alptekin, G. Cycle design and optimization of pressure swing adsorption cycles for pre-combustion CO_2 capture. *Appl. Energy* **2019**, *254*, 113624.

[33] Jiang, H.; Ebner, A. D.; Ritter, J. A. Importance of incorporating a vacuum pump performance curve in dynamic adsorption process simulation. *Ind. Eng. Chem. Res* **2020**, *59*, 856–873.

[34] Roussanaly, S.; Anantharaman, R.; Lindqvist, K.; Zhai, H.; Rubin, E. Membrane properties required for post-combustion CO_2 capture at coal-fired power plants. *J. Membr. Sci.* **2016**, *511*, 250 – 264.

[35] Haaf, M.; Anantharaman, R.; Roussanaly, S.; Ströhle, J.; Epple, B. CO_2 capture from waste-to-energy plants: Techno-economic assessment of novel integration concepts of calcium looping technology. *Resour. Conserv. Recycl.* **2020**, *162*, 104973.

[36] NETL, Quality guidelines for energy system studies: Cost estimation methodology for NETL assessments of power plant performance. 2011; `DOE/NETL-2011/1455`.

[37] Anantharaman, R.; Bolland, O.; Booth, N.; Dorst, E.; Ekstrom, C.; Franco, F.; Macchi, E.; Manzolini, G.; Nikolic, D.; Pfeffer, A.; Prins, M.; Rezvani, S.; Robinson, L. D1.4.3 European best practice guidelines for assessment of CO_2 capture technologies (DECARBit Project). 2011; `https://www.sintef.no/globalassets/project/decarbit/d-1-4-3_euro_bp_guid_for_ass_co2_cap_tech_280211.pdf`.

[38] U.S. Geological Survey, Cobalt & Nickel Statistics, in Kelly, T.D., and Matos, G.R., and comps., Historical statistics for mineral and material commodities in the United States (2013 version): U.S. Geological Survey Data Series 140. 2015; accessed June 26, 2020.

[39] Stöcker, J.; Whysall, M.; Miller, G. 30 Years of PSA Technology for Hydrogen Purification. UOP LLC, Des Plaines, IL, USA, 1998.

[40] Roussanaly, S. Calculating CO_2 avoidance costs of carbon capture and storage from industry. *Carbon Manage.* **2019**, *10*, 105–112.

[41] Gardarsdottir, S. O.; De Lena, E.; Romano, M.; Roussanaly, S.; Voldsund, M.; Pérez-Calvo, J.-F.; Berstad, D.; Fu, C.; Anantharaman, R.; Sutter, D.; Gazzani, M.; Mazzotti, M.; Cinti, G. Comparison of technologies for CO_2 capture from cement production—Part 2: Cost analysis. *Energies* **2019**, *12*, 542.

[42] Rajagopalan, A. K.; Rajendran, A. The effect of nitrogen adsorption on vacuum swing adsorption based post-combustion CO2 capture. *Int. J. Greenh. Gas Control* **2018**, *78*, 437 – 447.

[43] Deng, H.; Roussanaly, S.; Skaugen, G. Techno-economic analyses of CO_2 liquefaction: Impact of product pressure and impurities. *Int. J. Refrig.* **2019**, *103*, 301 – 315.

This is the accepted version of an article published in Separation and Purification Technology
http://dx.doi.org/10.1016/j.seppur.2020.117832

Supporting Information

Techno-economic Assessment of Optimised Vacuum Swing Adsorption for Post-Combustion CO_2 Capture from Steam-Methane Reformer Flue Gas

Sai Gokul Subraveti[1], Simon Roussanaly[2,*], Rahul Anantharaman[2], Luca Riboldi[2], and Arvind Rajendran[1,*]

[1] *Department of Chemical and Materials Engineering, University of Alberta, 12th floor, Donadeo Innovation Centre for Engineering (ICE), 9211-116 Street, Edmonton, Alberta T6G1H9, Canada*

[2] *SINTEF Energy Research, NO-7465, Trondheim, Norway*

[*] *Corresponding authors. E-mail: Simon.Roussanaly@sintef.no (Simon Roussanaly), arvind.rajendran@ualberta.ca (Arvind Rajendran)*

This is the accepted version of an article published in Separation and Purification Technology
http://dx.doi.org/10.1016/j.seppur.2020.117832

S1 Baseline MEA-based CO_2 capture

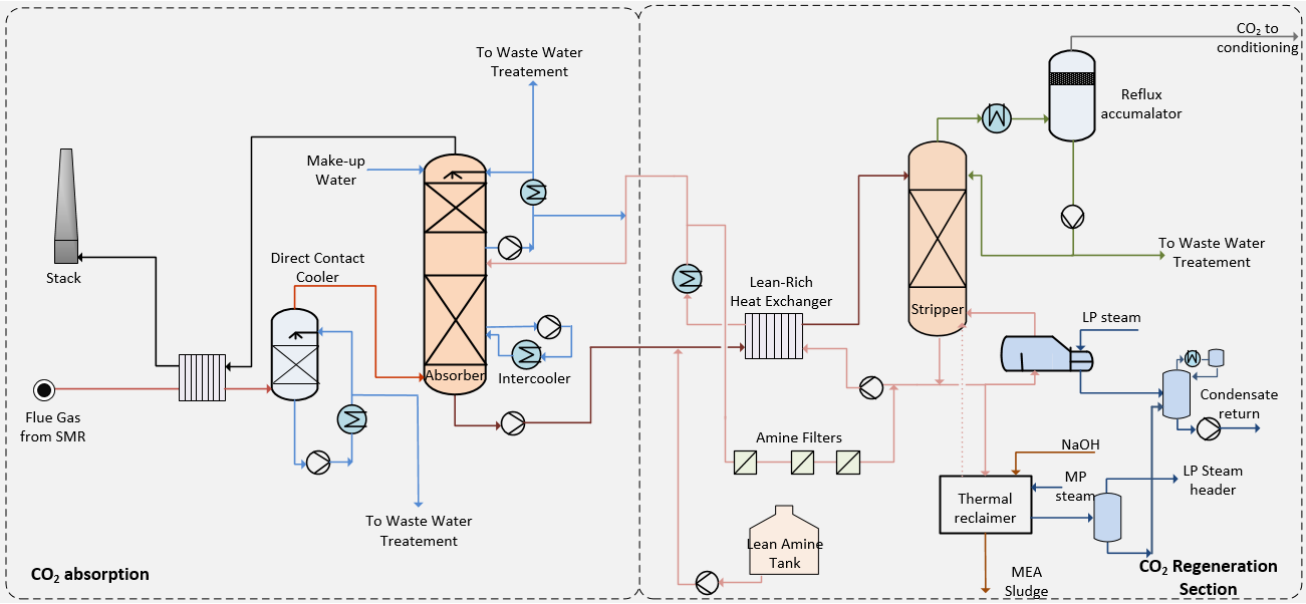

Figure S1: Detailed process flow diagram of the MEA-based CO_2 capture process for the hydrogen production plant with CO_2 capture [1].

This is the accepted version of an article published in Separation and Purification Technology
http://dx.doi.org/10.1016/j.seppur.2020.117832

Table S1: Key performances of hydrogen production plant without and with MEA-based CCS [2].

Parameter	**Without CCS**	**With CCS**
Natural Gas to feedstock (t h^{-1})	51.66	51.66
Natural Gas to fuel (t h^{-1})	26.59	26.59
Natural Gas LHV (MJ kg^{-1})	46.49	46.49
Total Energy Input (MW)	1010	1010
H_2 to battery limit (t h^{-1})	18.77	18.77
H_2 to battery limit (Nm^3 H_2 h^{-1})	208700	208700
Total energy in H_2 product (MW)	626	626
Gross power output from Steam cycle (MW_e)	123.8	91.6
H_2 plant and co-generation power consumption (MW_e)	-3.5	-3.5
CO_2 capture plant (MW_e)	-	-6.7
CO_2 conditioning plant (MW_e)	-	-18.3
Net Power output (MW_e)	120.3	63.1
Total energy in H_2 product compared Total Energy Input (%)	61.9	61.9
Total energy in H_2 and electricity produced compared Total Energy Input (%)	73.8	68.2
Emissions (kg_{CO_2} Nm^{-3} H_2)	0.994	0.100
Levelised Cost of Hydrogen (c€Nm^{-3} H_2)	12.20	18.07
CO_2 avoidance cost (€/$t_{CO_2,avoided}$)	-	66.6
CO_2 capture cost (€/$t_{CO_2,avoided}$)	-	30.1

This is the accepted version of an article published in Separation and Purification Technology
http://dx.doi.org/10.1016/j.seppur.2020.117832

S2 Adsorbent Materials

Table S2: Dual-site Langmuir isotherm parameters.

	Zeolite 13X [3]	**UTSA-16** [4]	**IISERP MOF2** [5]
CO_2			
q_{sb} (mol kg^{-1})	3.09	4.08	3.29
q_{sd} (mol kg^{-1})	2.54	1.29	1.89
b_0 (m^3 mol^{-1})	8.65×10^{-7}	2.52×10^{-7}	9.39×10^{-8}
d_0 (m^3 mol^{-1})	2.63×10^{-8}	1.75×10^{-9}	5.23×10^{-7}
ΔU_b (J mol^{-1})	-36641	-32800	-31135
ΔU_d (J mol^{-1})	-35690	-35040	-31135
N_2			
q_{sb} (mol kg^{-1})	3.09	1.33	3.29
q_{sd} (mol kg^{-1})	2.54	1.77	1.89
b_0 (m^3 mol^{-1})	2.69×10^{-6}	9.17×10^{-5}	2.55×10^{-7}
d_0 (m^3 mol^{-1})	2.69×10^{-6}	9.42×10^{-9}	2.55×10^{-7}
ΔU_b (J mol^{-1})	-15710	-7500	-11890
ΔU_d (J mol^{-1})	-15710	-27760	-11890

This is the accepted version of an article published in Separation and Purification Technology
http://dx.doi.org/10.1016/j.seppur.2020.117832

S3 Technical Modelling of Vacuum Swing Adsorption

S3.1 Model Equations

Component mass balance

$$\frac{\partial y_\mathrm{i}}{\partial t} + \frac{y_\mathrm{i}}{T}\frac{\partial P}{\partial t} - \frac{y_\mathrm{i}}{P}\frac{\partial T}{\partial t} = \frac{T}{P}D_\mathrm{L}\frac{\partial}{\partial z}\left(\frac{P}{T}\frac{\partial y_\mathrm{i}}{\partial z}\right) - \frac{T}{P}\frac{\partial}{\partial z}\left(\frac{y_\mathrm{i}P}{T}v\right) - \frac{RT}{P}\frac{1-\varepsilon}{\varepsilon}\frac{\partial q_\mathrm{i}}{\partial t} \tag{S1}$$

Total mass balance

$$\frac{1}{P}\frac{\partial P}{\partial t} - \frac{1}{T}\frac{\partial T}{\partial t} = -\frac{T}{P}\frac{\partial}{\partial z}\left(\frac{P}{T}v\right) - \frac{RT}{P}\frac{1-\varepsilon}{\varepsilon}\sum_{i=1}^{n_\mathrm{comp}}\frac{\partial q_\mathrm{i}}{\partial t} \tag{S2}$$

Linear driving force model

$$\frac{\partial q_\mathrm{i}}{\partial t} = k_\mathrm{i}(q_\mathrm{i}^* - q_\mathrm{i}) \tag{S3}$$

Mass transfer coefficient (macropore controlled)

$$k_\mathrm{i} = \frac{c_\mathrm{i}}{q_\mathrm{i}^*}\frac{15\varepsilon_\mathrm{p}D_\mathrm{p}}{r_\mathrm{p}^2} \tag{S4}$$

Column energy balance

$$\begin{aligned}\left[\frac{1-\varepsilon}{\varepsilon}\left(\rho_\mathrm{s}C_\mathrm{p,s} + C_\mathrm{p,a}\sum_{i=1}^{n_\mathrm{comp}}q_\mathrm{i}\right)\right]\frac{\partial T}{\partial t} &= \frac{K_\mathrm{z}}{\varepsilon}\frac{\partial^2 T}{\partial z^2} - \frac{C_\mathrm{p,g}}{R}\frac{\partial P}{\partial t} - \frac{C_\mathrm{p,g}}{R}\frac{\partial}{\partial z}(vP) \\ &\quad - \frac{1-\varepsilon}{\varepsilon}C_\mathrm{p,a}T\sum_{i=1}^{n_\mathrm{comp}}\frac{\partial q_\mathrm{i}}{\partial t} + \frac{1-\varepsilon}{\varepsilon}\sum_{i=1}^{n_\mathrm{comp}}\left(\Big(-\Delta H\Big)\frac{\partial q_\mathrm{i}}{\partial t}\right)\end{aligned} \tag{S5}$$

Pressure drop (Ergun's equation)

$$-\frac{\partial P}{\partial z} = \frac{150}{4}\frac{1}{r_\mathrm{p}^2}\Big(\frac{1-\varepsilon}{\varepsilon}\Big)^2\mu v + \frac{1.75}{2}\frac{1}{r_\mathrm{p}}\Big(\frac{1-\varepsilon}{\varepsilon}\Big)\rho|v|v \tag{S6}$$

Ideal gas law

$$c_\mathrm{i} = \frac{y_\mathrm{i}P}{RT} \tag{S7}$$

This is the accepted version of an article published in Separation and Purification Technology
http://dx.doi.org/10.1016/j.seppur.2020.117832

Table S3: Boundary conditions for the 4-step VSA cycle.

Step	z=0	z=L
Adsorption	$v\|_{z=0} = v_{\text{feed}}$	$P\|_{\text{z=L}} = P_{\text{H}}$
	$D_{\text{L}} \frac{\partial y_i}{\partial z}\big\|_{\text{z=0}} = -v\|_{\text{z=0}} \left(y_{i,\text{feed}} - y_i\|_{\text{z=0}}\right)$	$\frac{\partial y_i}{\partial z}\big\|_{\text{z=L}} = 0$
	$\frac{\partial T}{\partial z}\big\|_{\text{z=0}} = -\varepsilon\, v\|_{\text{z=0}}\, \rho_{\text{g}} C_{p,\text{g}} (T_{\text{feed}} - T\|_{\text{z=0}})$	$\frac{\partial T}{\partial z}\big\|_{\text{z=L}} = 0$
Blowdown	$\frac{\partial P}{\partial z}\big\|_{\text{z=0}} = 0$	$v\|_{\text{z=L}} = v_{\text{vac.pump}}$
	$\frac{\partial y_i}{\partial z}\big\|_{\text{z=0}} = 0$	$\frac{\partial y_i}{\partial z}\big\|_{\text{z=L}} = 0$
	$\frac{\partial T}{\partial z}\big\|_{\text{z=0}} = 0$	$\frac{\partial T}{\partial z}\big\|_{\text{z=L}} = 0$
Evacuation	$v\|_{\text{z=0}} = v_{\text{vac.pump}}$	$\frac{\partial P}{\partial z}\big\|_{\text{z=L}} = 0$
	$\frac{\partial y_i}{\partial z}\big\|_{\text{z=0}} = 0$	$\frac{\partial y_i}{\partial z}\big\|_{\text{z=L}} = 0$
	$\frac{\partial T}{\partial z}\big\|_{\text{z=0}} = 0$	$\frac{\partial T}{\partial z}\big\|_{\text{z=L}} = 0$
Light Product Pressurisation	$\frac{\partial P}{\partial z}\big\|_{\text{z=0}} = 0$	$v\|_{\text{z=L}} = \frac{v_{\text{ADS}} P_{\text{ADS}}\|_{\text{z=L}}}{P\|_{\text{z=L}}}$
	$\frac{\partial y_i}{\partial z}\big\|_{\text{z=0}} = 0$	$D_{\text{L}} \frac{\partial y_i}{\partial z}\big\|_{\text{z=L}} = -v\|_{\text{z=L}} \left(y_{i,\text{feed}} - y_i\|_{\text{z=L}}\right)$
	$\frac{\partial T}{\partial z}\big\|_{\text{z=0}} = 0$	$\frac{\partial T}{\partial z}\big\|_{\text{z=L}} = -\varepsilon\, v\|_{\text{z=L}}\, \rho_{\text{g}} C_{\text{pg}} (T_{\text{feed}} - T\|_{\text{z=L}})$

This is the accepted version of an article published in Separation and Purification Technology
http://dx.doi.org/10.1016/j.seppur.2020.117832

Table S4: VSA simulation parameters.

Parameter	Value
Column Properties	
Particle diameter, d_p (mm)	1.5
Column void fraction, ϵ_B (-)	0.37
Particle void fraction, ϵ_P (-)	0.35
Tortuosity, τ (-)	3
Operating Conditions	
Adsorption pressure, P_H (bar)	1.02
Inlet feed composition, y_{CO_2}/y_{N_2} (-)	0.2/0.8
Inlet feed temperature, T_{feed} (K)	298.15
Physical Properties	
Adsorbent density, ρ_s (kg m^{-3})	
Zeolite 13X	1130.0 [3]
UTSA-16	1171.0 [4]
IISERP MOF2	937.7 [5]
Molecular diffusivity, D_m (cm^2 s^{-1})	0.16
Fluid viscosity, μ (cP)	0.0172
Specific heat capacity of adsorbent, $C_{p,s}$ (J kg^{-1} K^{-1})	
Zeolite 13X	1070.0
UTSA-16	1070.0
IISERP MOF2	1070.0
Specific heat capacity of gas phase, $C_{p,g}$ (J mol^{-1} K^{-1})	30.7
Specific heat capacity of adsorbed phase, $C_{p,a}$ (J mol^{-1} K^{-1})	30.7
Inside heat transfer coefficient, h_{in} (J m^{-2} K^{-1} s^{-1})	0
Outside heat transfer coefficient, h_{out} (J m^{-2} K^{-1} s^{-1})	0
Effective gas thermal conductivity, K_z (J m^{-1} K^{-1} s^{-1})	0.09
Universal gas constant, R (m^3 Pa mol^{-1} K^{-1})	8.314

This is the accepted version of an article published in Separation and Purification Technology
http://dx.doi.org/10.1016/j.seppur.2020.117832

S3.2 Design of Unit Train

The procedure proposed by Khurana and Farooq [6] was used to determine the column scheduling. Each train comprises minimum number of columns and vacuum pumps necessary for a continuous operation. The minimum number of columns per train was calculated as follows:

$$N = \text{ceiling}\left(\frac{\sum_{i=\text{steps}} t_i}{t_{\text{ADS}}}\right) \tag{S8a}$$

t_i represents the duration of step i in the cycle. The minimum number of blowdown/evacuation vacuum pumps required is given by,

$$N_{\text{V},j} = \text{ceiling}\left(\frac{t_j}{t_{\text{ADS}}}\right) \quad j = \text{blowdown/evacuation} \tag{S8b}$$

If sum of the individual steps in a cycle is not a multiple of the adsorption time, an idle step has to be included after evacuation step so that the bed profiles are least affected [6]. The duration of an idle step was calculated as follows:

$$t_{\text{IDLE}} = N t_{\text{ADS}} - \sum_{i=\text{steps}} t_i \tag{S8c}$$

This is the accepted version of an article published in Separation and Purification Technology
http://dx.doi.org/10.1016/j.seppur.2020.117832

S3.3 Parallel Trains

A single VSA train might not be sufficient to treat the large volume of flue gas. Hence, several trains of VSA units in parallel are required to capture 90% CO_2 [6, 7]. The number of parallel trains can be calculated as:

$$M = \text{ceiling}\left(\frac{\dot{F}_{\text{flue}}}{\dot{F}_{\text{train}}}\right) \tag{S9}$$

Here $\dot{F}_{\text{flue}}$ is the total flue gas flow rate in kmol h^{-1} and $\dot{F}_{\text{train}}$ is the average molar flow rate of the feed to each train in kmol h^{-1}. It is worth mentioning that the inlet pressure varies over the duration of the adsorption step owing to the constant velocity boundary condition at the feed end. Therefore, the average molar flow rate of feed to each train was calculated based on an integral average of the molar flow rate over the duration of the adsorption step (shown in Eq. S10) and then, used to calculate the number of parallel trains.

$$\dot{F}_{\text{train}} = \frac{1}{t_{\text{ADS}}} \int_0^{t_{\text{ADS}}} \dot{F} dt \tag{S10}$$

This is the accepted version of an article published in Separation and Purification Technology
http://dx.doi.org/10.1016/j.seppur.2020.117832

S4 Technical Modelling of peripheral units

The implementation of CO_2 capture using VSA technology requires several peripheral units extending from flue gas pre-treatment to CO_2 conditioning. In this section, the technical modeling related to each component unit is discussed below.

Flue Gas Cooling and Drying: The wet flue gas was first cooled to 313.15 K by a direct contact cooler and then dehydrated using a molecular sieve 3Å [8].

Compressors: Single-stage compressors were modeled as an isoentropic compression process. The motor efficiency was assumed to be 100%. The energy consumption was calculated as follows:

$$E_{\mathrm{C}}\ (\mathrm{J_e}) = \frac{1}{\eta_{\mathrm{C}}} \frac{\gamma}{\gamma - 1} \int_{t=0}^{t=t_{\mathrm{ADS}}} QP \left[\left(\frac{P}{P_{\mathrm{ref}}} \right)^{\frac{\gamma-1}{\gamma}} - 1 \right] \mathrm{d}t \tag{S11a}$$

Here η_{C} is the compression efficiency which was assumed to be 80%, γ is the adiabatic constant obtained from a linear regression as a function of CO_2 composition (see Fig. S2), P is the pressure, P_{ref} is the reference pressure of flue gas, t_{ADS} is the adsorption step time and Q is the volumetric flow rate of the feed mixture.

Vacuum Pumps: The energy consumption by a vacuum pump was modeled as an isentropic expansion process as given by,

$$E_{\mathrm{V}}\ (\mathrm{J_e}) = \frac{1}{\eta_{\mathrm{V}}} \frac{\gamma}{\gamma - 1} \int_{t=0}^{t=t_{\mathrm{step}}} QP \left[\left(\frac{P_{\mathrm{atm}}}{P} \right)^{\frac{\gamma-1}{\gamma}} - 1 \right] \mathrm{d}t \tag{S11b}$$

In the above equation, t_{step} is the step duration of blowdown/evacuation step, η_{V} is the vacuum pump efficiency.

Heat Exchangers: Two identical counter-current heat exchangers were considered to cool the dry flue gas after compression to 298.15 K. The design was evaluated based on the cooling duty and the log-mean temperature difference (LMTD) for the counter-current flow. The dry flue gas represents the hot side of the heat exchangers while the cooling water is the cold side. To determine the cooling duty, input and output stream characteristics of the hot dry flue gas were used. While the mass flow rate, input and output temperatures of the dry flue gas were known,

This is the accepted version of an article published in Separation and Purification Technology
http://dx.doi.org/10.1016/j.seppur.2020.117832

the specific heat capacity was obtained from the National Institute of Standards and Technology (NIST) REFPROP v.9 database [9]. The mass flow rate of the cooling water was then determined by dividing the cooling duty by the heat capacity [9] and an allowable temperature increase of the cooling water. The inlet and outlet temperatures of cooling water were set to 283.15 K and 291.5 K, respectively. The heat exchanger area (A_{EX}) was obtained using,

$$A_{\mathrm{EX}} = \frac{\dot{Q}_{\mathrm{EX}}}{U_{\mathrm{EX}}\mathrm{LMTD}} \tag{S12}$$

where Q_{EX} is the cooling duty (W) and U_{EX} is the overall heat transfer coefficient which is assumed to be around 1000 W m^{-2} K^{-1} for all process heat exchangers [10].

CO_2 Conditioning: The CO_2 after capture undergoes compression from 1 bar, 298.15 K to offshore pipeline transport conditions at 200 bar and 318.15 K. The CO_2 conditioning before pipeline transport was modelled as a four-stage compression system with intercoolers and a pump to deliver the CO_2 at desired pressure in Aspen HYSYS. The readers are referred elsewhere [2] for detailed modeling of CO_2 conditioning.

CO_2 Transport and Storage: The costs of the transport and storage are assessed using the iCCS tool developed by SINTEF Energy Research [11] and previously documented [12–14]. The transport cost model relies on the pipeline cost model developed by Knoope et al. [15] and the storage cost model relies on the Zero Emission Platform for Zero Emission Fossil Fuel Power Plants [16].

This is the accepted version of an article published in Separation and Purification Technology
http://dx.doi.org/10.1016/j.seppur.2020.117832

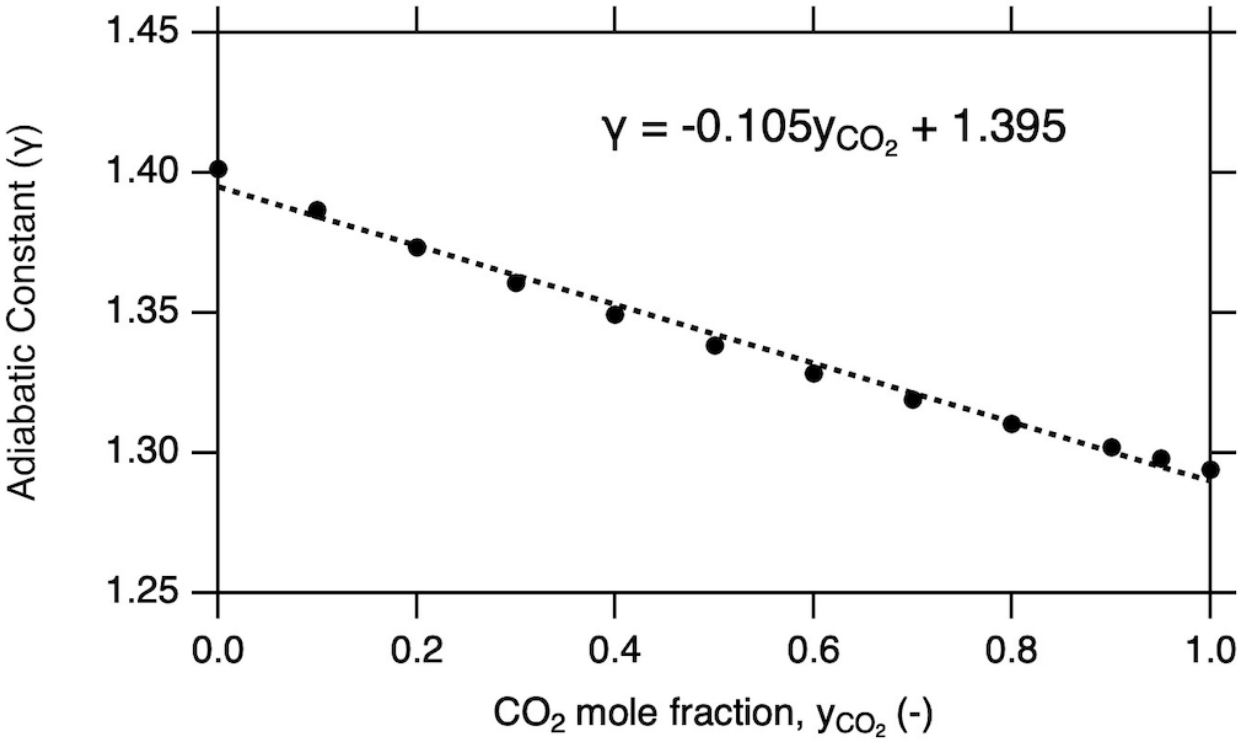

Figure S2: Linear dependence of adiabatic constant (γ) as a function of CO_2 mole fraction. Note that the γ values were obtained from NIST database [9].

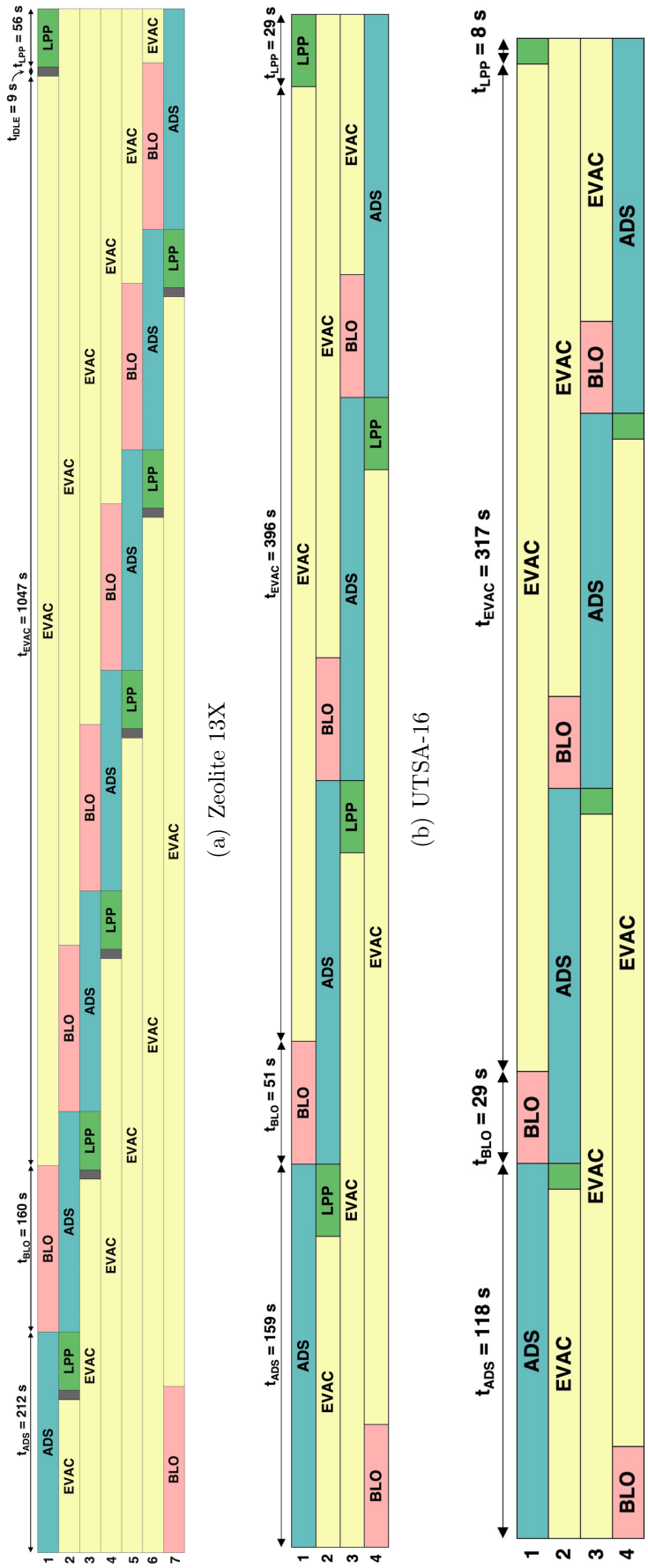

(a) Zeolite 13X

(b) UTSA-16

(c) HSERP MOF2

Figure S3: Optimal cycle schedules for all three adsorbents.

This is the accepted version of an article published in Separation and Purification Technology
http://dx.doi.org/10.1016/j.seppur.2020.117832

References

[1] IEAGHG, Techno-economic evaluation of SMR based standalone (merchant) plant with CCS, 2017/02. February 2017.

[2] Roussanaly, S.; Anantharaman, R.; Fu., C. Low-carbon footprint hydrogen production from natural gas: A techno-economic analysis of carbon capture and storage from steam-methane reforming. *Chem. Eng. Trans.* **2020** (Accepted).

[3] Haghpanah, R.; Majumder, A.; Nilam, R.; Rajendran, A.; Farooq, S.; Karimi, I. A.; Amanullah, M. Multiobjective optimization of a four-step adsorption process for postcombustion CO_2 capture via finite volume simulation. *Ind. Eng. Chem. Res* **2013**, *52*, 4249–4265.

[4] Agueda, V. I.; Delgado, J. A.; Uguina, M. A.; Brea, P.; Spjelkavik, A. I.; Blom, R.; Grande, C. Adsorption and diffusion of H_2, N_2, CO, CH_4 and CO_2 in UTSA-16 metal-organic framework extrudates. *Chem. Eng. Sci.* **2015**, *124*, 159 – 169.

[5] Burns, T. D.; Pai, K. N.; Subraveti, S. G.; Collins, S. P.; Krykunov, M.; Rajendran, A.; Woo, T. K. Prediction of MOF performance in vacuum swing adsorption systems for post-combustion CO_2 capture based on integrated molecular simulations, process optimizations, and machine learning models. *Environ. Sci. Technol.* **2020**, *54*, 4536–4544.

[6] Khurana, M.; Farooq, S. Integrated adsorbent process optimization for minimum cost of electricity including carbon capture by a VSA process. *AIChE J.* **2019**, *65*, 184–195.

[7] Susarla, N.; Haghpanah, R.; Karimi, I.; Farooq, S.; Rajendran, A.; Tan, L. S. C.; Lim, J. S. T. Energy and cost estimates for capturing CO_2 from a dry flue gas using pressure/vacuum swing adsorption. *Chem. Eng. Res. Des.* **2015**, *102*, 354 – 367.

[8] Roussanaly, S.; Anantharaman, R.; Lindqvist, K.; Hagen, B. A new approach to the identification of high-potential materials for cost-efficient membrane-based post-combustion CO_2 capture. *Sustain. Energy Fuels* **2018**, *2*, 1225–1243.

[9] Lemmon, E.; Huber, M.; McLinden, M. NIST standard reference database 23: Reference fluid thermodynamic and transport properties-REFPROP, Version 9.1. 2013.

This is the accepted version of an article published in Separation and Purification Technology
http://dx.doi.org/10.1016/j.seppur.2020.117832

[10] Deng, H.; Roussanaly, S.; Skaugen, G. Techno-economic analyses of CO_2 liquefaction: Impact of product pressure and impurities. *Int. J. Refrig.* **2019**, *103*, 301 – 315.

[11] Jakobsen, J.; Roussanaly, S.; Anantharaman, R. A techno-economic case study of CO_2 capture, transport and storage chain from a cement plant in Norway. *J. Clean. Prod.* **2017**, *144*, 523 – 539.

[12] Roussanaly, S.; Brunsvold, A. L.; Hognes, E. S. Benchmarking of CO_2 transport technologies: Part II – Offshore pipeline and shipping to an offshore site. *Int. J. Greenh. Gas Control* **2014**, *28*, 283 – 299.

[13] Roussanaly, S.; Grimstad, A.-A. The Economic value of CO_2 for EOR applications. *Energy Procedia* **2014**, *63*, 7836 – 7843.

[14] Skaugen, G.; Roussanaly, S.; Jakobsen, J.; Brunsvold, A. Techno-economic evaluation of the effects of impurities on conditioning and transport of CO_2 by pipeline. *Int. J. Greenh. Gas Control* **2016**, *54*, 627 – 639.

[15] Knoope, M.; Guijt, W.; Ramírez, A.; Faaij, A. Improved cost models for optimizing CO_2 pipeline configuration for point-to-point pipelines and simple networks. *Int. J. Greenh. Gas Control* **2014**, *22*, 25 – 46.

[16] European Technology Platform for Zero Emission Fossil Fuel Power Plants (ZEP), The costs of CO_2 storage, post-demonstration CCS in the EU, Brussels, Belgium. 2011.

This is the accepted version of an article published in Separation and Purification Technology
http://dx.doi.org/10.1016/j.seppur.2020.117832